![TÉCNICO LISBOA]

A numerical study of the Dirac Spectrum and Transmission Problems employing the Method of Fundamental Solutions

Francisco Alves Bento

Thesis to obtain the Master of Science Degree in

Applied Mathematics and Computation

Supervisors: Pedro Ricardo Simão Antunes
Juha Hans Videman

Examination Committee

Chairperson: Prof. Pedro Lima
Members of the Committee: Prof. Hugo Tavares
Prof. Pedro Serranho

September 2023

Acknowledgments

Abstract

Keywords

Resumo

Palavras Chave

Contents

List of Figures

x

List of Tables

List of Algorithms

Listagens

Acronyms

1

Introduction

Contents

Partial Differential Equations (PDEs) are one of the most powerful mathematical techniques in mathematical modelling, with direct applications in engineering, physics and even machine learning. As such, the development of reliable numerical methods to solve them are of major importance since most of these equations cannot be solved analytically. Throughout this work we are going to explore a newly developed class type of numerical methods known as *meshless* or *meshfree* methods and its applications in open problems in mathematical-physics. Contrary to the widely used classical methods like finite differences and finite element methods which involve some previously created mesh (where numerically solving a PDE might be difficult if the domain's geometry is convoluted), these type of meshless methods are easier to use since they are mostly independent from the domain, at least from an implementation point of view.

The meshless method we are interested in is known as the Method of Fundamental Solutions (MFS) that is based on the fundamental solutions of well-known equations such as the Laplace Equation and the Helmholtz equation. As we are going to see, such set of functions have some interesting properties that we can use to numerically solve PDEs. We are also going to implement a generalization of MFS based on *Kansa method*, another meshless method that in turn uses radial basis functions.

One of the main points of this work is to address open conjectures related with the spectrum of the Dirac Operator while seeking numerical evidence of some proposed isoperimetric inequalities using the methods listed above. Motivated by developments in molecular and nuclear physics, and the particularly interesting properties of low energy charge carriers in graphene, Dirac equation replaced the non-relativistic Schrödinger Equation. Unfortunately, the matrix structure found in the Dirac Equation makes it harder to study. The interest in capable numerical methods arises in such conditions: not only can they be used to test some conjectures but they can also be a source of insights for future advances.

1.1 Thesis Overview

2

Some Preliminary Results

Contents

2.1 Some concepts on Banach Spaces

This section begins by introducing preliminary concepts on Banach Spaces, which play a crucial role in the subsequent numerical methods to be presented. For more details see [2] or [3]. Consider a field $\mathbb{F}$ ($\mathbb{R}$ or $\mathbb{C}$). We say that a vector space E is a *normed space* if there exists a map $\|\cdot\|$ (called a *norm*) over $\mathbb{F}$ such that

1. $\|\alpha x\| = |\alpha|\|x\|$, $\alpha \in \mathbb{F}$, $\forall x \in E$;

2. $\|x + y\| \leq \|x\| + \|y\|$, $\forall x, y \in E$;

3. $\|x\| \geq 0$, $\forall x \in E$;

4. $\|x\| = 0 \iff x = 0$.

In particular, a pivotal notion is of *Banach spaces*, i.e, E is a Banach space if it is a complete normed space.

Definition 2.1.1. *Consider a linear operator $T : E \to F$, where E and F are Banach spaces with the associated norms $\|\cdot\|_E$ and $\|\cdot\|_F$, respectively. Then*

1. *The **nullspace** (also called the **kernel**) of T is a subset of E such that*

$$N(T) = \{x \in E : Tx = 0\}.$$

   *Accordingly, the **range** (also called the **image**) of T is a subset of F such that*

$$R(T) = \{y \in F : \text{ there exists some } x \in E \text{ such that } y = Tx\}.$$

2. *T is said to be **bounded** (continuous) if there exists $C > 0$ such that $\|Tx\|_F \leq C\|x\|_E$. We define the norm of the operator T as*

$$\|T\| = \sup_{\substack{x \in E \\ x \neq 0}} \frac{\|Tx\|_F}{\|x\|_E}.$$

   In this case we write $T \in \mathcal{L}(E, F)$. If $E = F$, we write $T \in \mathcal{L}(E)$;

3. *The space of linear and continuous maps from E to $\mathbb{R}$ is the **dual space** of E denoted by $E^\star$. If $S \in E^\star$, its norm (the dual norm) is defined in the same manner as the operator norm above, i.e.*

$$\|S\| = \sup_{\substack{x \in E \\ x \neq 0}} \frac{|\langle S, x \rangle|}{\|x\|}$$

where $\langle S, x \rangle_{E^\star, E} = Sx$ and denotes de duality pairing between $E^\star$ and E. As we will see below, it generalizes the notion of inner product in inner product spaces. Whenever it is obvious what dual pairing is being considered we just write $\langle \cdot, \cdot \rangle$;

4. *Assuming that T is bounded, T is said to be* **compact** *if for any bounded sequence $(u_n)_{n \in \mathbb{N}} \subset E$ there exists a subsequence $(u_{n_k})_{k \in \mathbb{N}}$ such that $(Tu_{n_k})_{k \in \mathbb{N}}$ converges in F;*

5. *Assume that the domain of T, which we represent by $\mathrm{Dom}(T)$, is dense in E. We say that the linear operator $T^\star : \mathrm{Dom}(T^\star) \subset F^\star \to E^\star$ is the* **adjoint** *of T if*

$$\langle v, Tu \rangle_{F^\star, F} = \langle T^\star v, u \rangle_{E^\star, E^\star}, \ \forall v \in \mathrm{Dom}(T^\star),$$

where the domain of $T^\star$ is defined by

$$\mathrm{Dom}(T^\star) = \{v \in F^\star : \exists c \geq 0 \text{ such that } |\langle v, Tu \rangle_{F^\star, F}| \leq c\|u\|, \ \forall u \in \mathrm{Dom}(T)\}.$$

The main result of this section concerns the dual of a normed space. In reality, we do not need to assume that E is a Banach space to present the next results. However, throughout this work, every normed space is also complete. We refer to Chapters 1 and 3 from [3].

Definition 2.1.2 (Reflexive space)**.** *Let E be a normed space and denote its dual by $E^\star$. The bidual space $E^{\star\star}$ is the dual of $E^\star$ with the associated norm*

$$\|\xi\| = \sup_{\substack{f \in E^\star \\ f \neq 0}} \frac{|\langle \xi, f \rangle|}{\|f\|}.$$

If the (canonical) map $J : E \to E^{\star\star}$ defined by

$$\langle Jx, f \rangle_{E^{\star\star}, E^\star} = \langle f, x \rangle_{E^\star, E}, \ \forall x \in E, \forall f \in E^\star$$

is surjective then E is said to be reflexive.

The definition above is an important detail to the justification of the Method of Fundamental Solutions. The main ingredient to justify this numerical method is the Hahn-Banach theorem.

Theorem 2.1.3 (Analytical form of Hahn-Banach Theorem)**.** *Let E be a normed space and $p : E \to \mathbb{R}$ a functional satisfying*

$$p(\lambda x) = \lambda p(x), \ \forall x \in E, \ \lambda > 0$$
$$p(x + y) \leq p(x) + p(y)$$

Let $G \subset E$ be a linear subspace and $g : G \to \mathbb{R}$ a linear functional such that

$$g(x) \leq p(x), \ \forall x \in G.$$

Then, there exists a linear functional $f : E \to \mathbb{R}$ that extends g to E, agrees with g on G, i.e, $f(x) = g(x), \ \forall x \in G$ and also satisfies

$$f(x) \leq p(x) \ \forall x \in E.$$

Remark 2.1.4. *The theorem mentioned above holds particular significance in Functional Analysis as it demonstrates that the dual $E^\star$ of a normed space E possesses interesting properties that warrant further study to gain a better understanding of the underlying space E. It can even be utilized to identify, although not uniquely, elements in both E and its dual $E^\star$ through the duality pairing. This result bears resemblance to the desirable properties exhibited by Hilbert spaces, which we will explore further in this work. It is beneficial to establish density when working with the dual pairing between a Banach space and its dual. However, it is important to note that the existence of the functional f is not explicitly provided, as the proof of Theorem (2.1.3) relies on the Axiom of Choice (Zorn's Lemma).*

Under some conditions, an interesting consequence of Theorem (2.1.3) is that two disjoint (and non-empty) convex sets can always be separated by a hyperplane in an infinite-dimensional space.

Definition 2.1.5. *Let E be a normed space, f a linear functional on E, and $c \in \mathbb{R}$. An hyperplane H is a subset of E of the form*

$$H = \{x \in E : \langle f, x \rangle = c\}.$$

Proposition 2.1.6. *Let H be a hyperplane defined by the equation $\langle f, x \rangle = c$, for some linear functional f and $c \in \mathbb{R}$. Then, H is closed if and only if f is continuous.*

Notice that if H is a closed hyperplane then the linear functional f that defines the hyperplane is an element of $E^\star$.

Definition 2.1.7. *Let A and B be two subsets of E. We say that a hyperplane H defined by the equation $\langle f, x \rangle = c$, for some linear functional f and $c \in \mathbb{R}$, strictly separates A and B if*

$$\langle f, x \rangle < c, \ \forall x \in A,$$

$$\langle f, x \rangle > c, \ \forall x \in B$$

Theorem 2.1.8 (Second geometric form of Hahn-Banach Theorem)**.** *Let A and B be two disjoint, non-empty and convex subsets of E such that A is closed and B is compact. Then, there exists a closed hyperplane that strictly separates A and B, i.e, there exists $f \in E^\star$ and $c \in \mathbb{R}$ such that for every $a \in A$*

and $b \in B$

$$\langle f, a \rangle < c < \langle f, b \rangle.$$

The following Lemma is a consequence of Theorem (2.1.8), and it is a useful tool to prove that some linear subspace $M \subset E$ is dense (in E). We start by introducing the notion of orthogonality of sets in Banach spaces with respect to the duality pairing.

Definition 2.1.9. *Let E be a Banach Space and M be a linear subspace of E. We define the orthogonal of M in E is respect to the duality pairing as*

$$M^{\perp} = \{\psi \in E^{\star} : \langle \psi, \varphi \rangle = 0, \ \forall \varphi \in M\}.$$

Accordingly, if $N \subset E^{\star}$ is a linear subspace, its orthogonal is defined as

$$N^{\perp} = \{\varphi \in E : \langle \psi, \varphi \rangle = 0, \ \forall \psi \in N\}$$

Lemma 2.1.10. *Let M and N in the same conditions of the definition above. Then*

$$(M^{\perp})^{\perp} = \overline{M}$$

and

$$\overline{N} \subset (N^{\perp})^{\perp}.$$

In particular, if E is a reflexive Banach space then

$$(N^{\perp})^{\perp} = \overline{N}.$$

Proof. Since $(M^{\perp})^{\perp} \subset E$ and $(N^{\perp})^{\perp} \subset E^{\star}$ are closed sets, by definition $M \subset (M^{\perp})^{\perp}$ and $N \subset (N^{\perp})^{\perp}$ the inclusions

$$\overline{M} \subseteq (M^{\perp})^{\perp}, \qquad \overline{N} \subseteq (N^{\perp})^{\perp}$$

follow. To check that $(M^{\perp})^{\perp} \subseteq \overline{M}$ we argue by contradiction. Let $x_0 \in (M^{\perp})^{\perp}$ such that $x_0 \notin \overline{M}$. Then, by Theorem (2.1.8) there exists a hyperplane with equation $\langle f, x \rangle = c$ for some $f \in E^{\star}$ and $c \in \mathbb{R}$ that strictly separates the sets $\{x_0\}$ and $\overline{M}$ (both are obviously non-empty convex sets). In particular,

$$\langle f, x \rangle_{E^{\star}, E} < c < \langle f, x_0 \rangle_{E^{\star}, E}, \ \forall x \in M.$$

Since M is a linear subspace, then $\langle f, x \rangle = 0, \ \forall x \in M$ since, otherwise, given any $x \in M$ we would

have that

$$\alpha\langle f, x\rangle_{E^\star, E} = \langle f, \alpha x\rangle_{E^\star, E} < c, \ \forall \alpha \in \mathbb{R}$$

which can only be possible if $\langle f, x\rangle_{E^\star, E} = 0$. Therefore, $f \in M^\perp$ and $\langle f, x_0\rangle_{E^\star, E} > 0$ but that is a contradiction since, by hypothesis, $x_0 \in (M^\perp)^\perp$ and $\langle f, x_0\rangle_{E^\star, E} = 0, \ \forall f \in M^\perp$.

To prove that $(N^\perp)^\perp = \overline{N}$, we use the same type of argument. Let $f_0 \in (N^\perp)^\perp$ such that $f_0 \notin \overline{N}$. Once again, there exists a hyperplane with equation $\langle \xi, f\rangle = c$ for some $\xi \in E^{**}$ and $c \in \mathbb{R}$ that strictly separates $\{f_0\}$ and $\overline{N}$, that is

$$\langle \xi, f\rangle < c < \langle \xi, f_0\rangle, \ \forall f \in N.$$

Since N is a linear subspace we can also conclude that $\langle \xi, f\rangle = 0, \forall f \in N$ and $\langle \xi, f_0\rangle > 0$. In order to get a contradiction, like in the case above, since E is a reflexive space, then the canonical map J defined in (2.1.2) is surjective, and we can write

$$\langle \xi, f_0\rangle_{E^{**}, E^\star} = \langle Jx_0, f_0\rangle_{E^{**}, E^\star} = \langle f_0, x_0\rangle_{E^\star, E}$$

for some $x_0 \in E$. If we can prove that $\langle f_0, x_0\rangle_{E^\star, E} = 0$, then the contradiction follows. Since $f_0 \in (N^\perp)^\perp$, then $\langle f_0, x_0\rangle_{E^\star, E} = 0$ if $x_0 \in N^\perp$, i.e, $\langle f, x_0\rangle_{E^\star, E} = 0, \forall f \in N$. Let $f \in N$. Then, by reflexivity,

$$\langle f, x_0\rangle_{E^\star, E} = \langle Jx_0, f\rangle_{E^{**}, E^\star} = \langle \xi, f\rangle_{E^{**}, E^\star} = 0, \ \forall f \in N$$

as we saw above (N is a linear subspace). The desired result follows. $\qquad\square$

Remark 2.1.11. *The result above will be useful to justify the Method of Fundamental Solutions. To prove that some subset N of a Banach Space E is dense it will suffice to show that its orthogonal $N^\perp$ only contains the trivial element, which belongs to both E and $E^\star$.*

2.2 Some concepts on Hilbert Spaces

In this section we introduce some complementary results in Hilbert spaces. Once again, for more details, see [2], [3] or [4]. Consider the field $\mathbb{F}$ ($\mathbb{R}$ or $\mathbb{C}$). We say that a vector space H is an *inner product space* (or a Pre-Hilbert space) if there exists a map $(\cdot, \cdot)$ (called an *inner product*) over $\mathbb{F}$ such that

1. $(x, y) = \overline{(y, x)}$ (The bar denotes complex conjugation if $\mathbb{F} = \mathbb{C}$);

2. $(x + y, z) = (x, z) + (y + z)$;

3. $(\alpha x, y) = \alpha(x, y), \ \alpha \in \mathbb{F}$;

4. $(x, x) \geq 0, \ \forall x \in H$;

5. $(x, x) = 0 \iff x = 0$.

Given $x, y \in H$, we say that x and y are orthogonal (denoted by $x \perp y$) if $(x, y) = 0$. Accordingly, given $E, F \subset H$, if $x \perp y$ for every $x \in E, y \in F$ then we say that E and F are orthogonal, $E \perp F$. We also denote by $E^\perp$ the set of all $y \in H$ that are orthogonal to every $x \in E$, i.e, $E^\perp = \{y \in H : (x, y) = 0, \ \forall x \in E\}$ which we call the orthogonal complement of E. We recall that every inner product space is also a normed space, where the inner product induces the norm

$$\|x\| = \sqrt{(x, x)}$$

satisfying the Cauchy-Schwarz inequality

$$|(x, y)| \leq \|x\| \, \|y\| \, , \ x, y \in H.$$

Finally, if the normed space is complete for the induced norm, then we say that it is a Hilbert space. In what follows, H will always denote a Hilbert space.

Example 2.2.1. *A very classical Hilbert space, which is going to be used throughout all of this work, is the space of square-integrable real-valued functions in an open and bounded subset Ω of $\mathbb{R}^d$, which is denoted by $L^2(\Omega)$ with the inner product given by*

$$(f, g)_{L^2(\Omega)} = \int_\Omega f(x) g(x) dx.$$

If considering complex-valued functions, the inner product is given by

$$(f, g)_{L^2(\Omega)} = \int_\Omega f(x) \overline{g}(x) dx,$$

where a bar over an expression represents the complex conjugate of the scalar (function).

While working within the framework of Hilbert spaces, proving the density of a subspace $M \subset H$ is more intuitive and can be derived straightforwardly. It may be of interest to the reader to compare the following results with Definition (2.1.9) and Lemma (2.1.10).

Theorem 2.2.2. *Consider a closed subspace $M \subset H$. Then,*

$$H = M \oplus M^\perp.$$

In other words, every $u \in H$ admits a unique decomposition $u = v + w$, where $v \in M$ and $w \in M^\perp$.

Corollary 2.2.3. *Consider a subspace $M \subset H$. Then M is dense in H if and only if $M^\perp = \{0\}$.*

Proof. Let $T = \overline{M}$. We want to prove that $T = H$. Using Theorem 2.2.2, it suffices to check that $T^\perp = \{0\}$. Since the inner product is continuous, then $T^\perp = M^\perp = \{0\}$.

On the other hand, since by definition T is closed, by Theorem 2.2.2 we have that $H = T \oplus T^\perp = T \oplus \{0\} = T$ as we wished. $\qquad\square$

A surprising property in Hilbert spaces is the fact that every linear and continuous function $T : H \to \mathbb{F}$ can be *represented* by some unique element in H. In what follows we assume that $\mathbb{F} = \mathbb{R}$.

Theorem 2.2.4 (Riesz Representation Theorem)**.** *Let $T : H \to \mathbb{R}$ be a linear and continuous functional. Then, there exists a unique $u \in H$ such that*

$$Tv = (u, v), \ \forall v \in H.$$

Moreover, let $H^\star$ be the dual space of H, that is, the space of all linear and continuous function from H to $\mathbb{R}$. Then the map $H^\star \mapsto H$ is an isometric isomorphism (which we denote by $\cong$) where

$$\|u\|_H = \|T\|_{H^\star}.$$

Remark 2.2.5. *Notice how the inner product in Hilbert spaces has replaced the duality pairing defined for Banach spaces. In fact, in a certain sense, Riesz Representation Theorem (2.2.4) allows us to make a stronger statement regarding the dual spaces of Hilbert spaces and work in a more natural framework without ever resorting to the Hahn-Banach Theorem (2.1.3). For example, it is interesting to observe that the definition of orthogonality and orthogonal subspaces in Hilbert spaces (via the inner product) and Banach spaces (via the duality pairing) are essentially the same, with the distinction being an isomorphism between the Hilbert space and its dual. However, in certain cases, working with the definition of orthogonality in Banach spaces can be more useful as it allows for better generalization, such as when proving the density of a closed subspace.*

A more general and useful result in our work is the Lax-Milgram Theorem.

Definition 2.2.6. *We say that a bilinear form $a : H \times H \to \mathbb{R}$ is continuous and coercive if*

- $|a(u, v)| \leq C \|u\| \|v\|, \ \forall u, v \in H$
- $a(u, u) \geq \alpha \|u\|^2, \ \forall u \in H$

respectively.

Theorem 2.2.7 (Lax-Milgram Theorem)**.** *Let $a(u, v)$ be a bilinear, continuous and coercive bilinear form on H. If T is a linear and continuous functional in H, then there exists a unique $u \in H$ such that*

$$a(u, v) = T(v), \ \forall v \in H.$$

In this section the well-known *Spectral Theorem* and the *Fredholm Alternative* are presented. With this in mind, we will now present key results and concepts (without proofs) that will provide the necessary foundation for stating the theorems.

Definition 2.2.8. *A sequence $(e_n)_{n \in \mathbb{N}} \in H$ is a Hilbert basis of H if*

1. $(e_n, e_m) = \begin{cases} 1, & n = m \\ 0, & n \neq m \end{cases}$ *;*

2. $\overline{\text{span}\{(e_n)_{n \in \mathbb{N}}\}} = H.$

In a sense, a Hilbert basis resembles a basis in a finite-dimensional vector space.

Proposition 2.2.9. *Let $(e_n)_{n \in \mathbb{N}}$ be a Hilbert basis of H. Then, for every $u \in H$, we can write*

$$u = \sum_{k \in \mathbb{N}} (u, e_k) e_k \quad \text{and} \quad \|u\|^2 = \sum_{k \in \mathbb{N}} |(u, e_k)|.$$

The last equality is known as Parseval's identity.

The proposition above is particularly interesting because it allows us to express every element of H in terms of a countable basis. The following result guarantees the existence of a Hilbert basis if certain conditions are met.

Definition 2.2.10. *We say that H is a separable Hilbert space if there exists a countable subset $M \subset H$ such that $\overline{M} = H$.*

Theorem 2.2.11. *Every separable Hilbert space admits an orthonormal Hilbert basis.*

We now present some properties that our operators must satisfy in order to state the Spectral Theorem.

Definition 2.2.12. *Consider a linear operator $T : H_1 \to H_2$, where H_1 and H_2 are Hilbert spaces.*

*1. Assume that $H = H_1 = H_2$ and $T \in \mathcal{L}(H)$. We say that $T^\star$ is the **adjoint** of T if*

$$(y, Tx) = (T^\star y, x), \ \forall x, y \in H;$$

*If $T = T^\star$, i.e, if T and $T^\star$ domains (and their image) coincide we say that T is **self-adjoint**.[1]*

*2. As above, let $T \in \mathcal{L}(H)$. We say that λ is an **eigenvalue** of T if $N(T - \lambda I) \neq \{0\}$. In that case we say that $\lambda \in \sigma(T)$ where $\sigma(T)$ is called the **spectrum** of T.[2] We also say that u is an **eigenvector** associated with the eigenvalue λ if $u \in N(T - \lambda I) \setminus \{0\}.$*

---

[1]The existence and uniqueness of $T^\star$ may not be obvious, but if follows from Riesz Representation Theorem (2.2.4). In any case, notice the similarities between this definition and the one given in Definition (2.1.1). In fact, in Banach spaces, the existence of the adjoint also comes from the Hahn-Banach Theorem (2.1.3)!

[2]Remarkably, in the infinite dimensional case, the set of eigenvalues $EV(T)$ may not coincide with the spectrum $\sigma(T)$. $T - \lambda I$ may fail to be invertible even if $T - \lambda I$ is injective.

We can derive some important properties regarding the spectrum of a compact operator and the spectrum of self-adjoint operators.

Proposition 2.2.13. *Let H be a Hilbert space and consider a compact operator $T \in \mathcal{L}(H)$. Then,*

- *$0 \in \sigma(T)$;*

- *one of the following holds:*

  - *$\sigma(T) = \{0\}$;*

  - *$\sigma(T) \setminus \{0\}$ is a finite set;*

  - *$\sigma(T) \setminus \{0\}$ is a sequence converging to 0.*

Proposition 2.2.14. *Let H be a Hilbert space and consider a self-adjoint operator $T \in \mathcal{L}(H)$. In this conditions, $\sigma(T)$ is real and eigenvectors corresponding to distinct eigenvalues are orthogonal.*

It is now possible to state on of the main results of this section.

Theorem 2.2.15 (Spectral Theorem for compact and self-adjoint operators)**.** *Let H be a separable Hilbert space of infinite dimension and let $T \in \mathcal{L}(H)$ be a compact self-adjoint operator. Then, H admits a Hilbert basis $(e_n)_{n \in \mathbb{N}}$ such that*

$$Te_n = \lambda_n e_n$$

for $\lambda_n \in \mathbb{R}$, $\lambda_n \to 0$ as $n \to \infty$, where λ_n can be assumed to be a decreasing sequence.

2.3   Lebesgue and Sobolev Spaces

In this section, we apply the results and concepts from the previous ones. Besides the usual references already presented, we recommend [5], [6] and [7]. Let $\Omega \subset \mathbb{R}^d$ be an open set. Consider a *multi-index* $\alpha = (\alpha_1, \ldots, \alpha_d) \in \mathbb{N}_0^d$, where $|\alpha| = \alpha_1 + \cdots + \alpha_d$. Given a function defined in Ω, we denote its partial derivatives of order α by

$$D^\alpha = \frac{\partial^{|\alpha|}}{\partial x_1^{\alpha_1} \ldots \partial x_d^{\alpha_d}}.$$

As usual, we denote the space of test functions with compact support in Ω by

$$\mathcal{D}(\Omega) = C_0^\infty(\Omega) = \{\varphi \in C^\infty(\Omega) : \operatorname{supp} \varphi \text{ is compact in } \Omega\}.$$

Definition 2.3.1 (Lebesgue spaces)**.** *Let $1 \leq p \leq \infty$. We define the Lebesgue space (L^p space)*

$$L^p(\Omega) = \left\{ u : \Omega \to \mathbb{R} : u \text{ is measurable and } \int_\Omega |f|^p < \infty \right\}$$

with the associated norm

$$\|f\|_{L^p(\Omega)} = \left(\int_\Omega |f|^p \right)^{\frac{1}{p}}.$$

If $p = \infty$ we set

$$L^\infty(\Omega) = \left\{ u : \Omega \to \mathbb{R} : u \text{ is measurable and } \exists C > 0 : |f(x)| \leq C \text{ a.e on } \Omega \right\}$$

with the associated norm

$$\|f\|_{L^\infty(\Omega)} = \inf\{C : |f(x)| \leq C \text{ a.e on } \Omega\}$$

Definition 2.3.2. *We say that $f \in L^1_{loc}(\Omega)$ if f is integrable in every compact $K \subset \Omega$, i.e.*

$$f\chi_K \in L^1(\Omega), \ \forall K \subset \Omega \text{ compact.}$$

This definition can be extended accordingly to every $L^p(\Omega)$ space, with $1 \leq p \leq \infty$.

Before introducing the notion of weak derivative in Sobolev spaces, it will be useful to dive into some Distribution theory. Consider the space of test functions $\mathcal{D}(\Omega)$ above. While we are not interested to define a topology in this space, we want to define linear and continuous functionals acting on $\mathcal{D}(\Omega)$. For now, it suffices to define (sequential) convergence in $\mathcal{D}(\Omega)$.

Definition 2.3.3. *Let $(\varphi_n)_n \in \mathcal{D}(\Omega)$ and $\varphi \in \mathcal{D}(\Omega)$. If*

1. *$\forall n \in \mathbb{N}$ there exists a compact $K \subseteq \Omega$ such $\operatorname{supp} \varphi_k \subseteq K$;*

2. *$\forall \alpha \in \mathbb{N}_0^d$ $\lim_n \|D^\alpha \varphi_n - D^\alpha \varphi\|_{L^\infty(\Omega)} = 0$*

then we say that φ_n converges to φ in $\mathcal{D}(\Omega)$.

Definition 2.3.4 (Space of distributions)**.** *The dual space of $D(\Omega)$, denoted by $\mathcal{D}^\star(\Omega)$, is called the space of distributions, and we say that $T \in \mathcal{D}^\star$ is a distribution.*

A very illustrative example, with consequences when defining the duality pairing in Sobolev spaces, is that any locally integrable function $u \in L^1_{loc}(\Omega)$ defines a distribution. In fact, it is easy to prove that the operator T_u defined by

$$T_u : \mathcal{D}(\Omega) \to \mathbb{R}$$
$$\varphi \mapsto \int_\Omega u\varphi$$

is linear and continuous. Therefore, one can give meaning to the action of a distribution over a test function, whenever the distribution is induced by a locally integrable function u. In this case, we can

write

$$\langle u, \varphi \rangle_{D^\star(\Omega), D(\Omega)} = \int_\Omega u\varphi$$

where the duality pairing $\langle \cdot, \cdot \rangle_{D^\star(\Omega), D(\Omega)}$ can be seen as a generalization of the $L^2(\Omega)$ inner product.

Definition 2.3.5 (Sobolev Spaces). *For $k \in \mathbb{N}$ and $1 \leq p \leq \infty$ we define the Sobolev space*

$$W^{k,p}(\Omega) = \{u \in L^p(\Omega) : D^\alpha u \in L^p(\Omega), \forall \alpha \in \mathbb{N}_0^d : |\alpha| \leq k\}$$

with the associated norms

- $1 \leq p < \infty$,

$$\|u\|_{W^{k,p}(\Omega)} := \left(\sum_{|\alpha| \leq k} \|D^\alpha u\|_{L^p(\Omega)}^p \right)^{\frac{1}{p}};$$

- $p = \infty$,

$$\|u\|_{W^{k,p}(\Omega)} := \max_{|\alpha| \leq k} \|D^\alpha u\|_{L^\infty(\Omega)}.$$

We say that $D^\alpha u$ is the weak derivative of order α of $u \in L^p(\Omega)$ if $D^\alpha u \in L^p(\Omega)$. The operator D^α is well-defined as a distribution, and satisfies

$$\int_\Omega D^\alpha u\varphi = (-1)^{|\alpha|} \int_\Omega u D^\alpha \varphi, \ \forall \varphi \in \mathcal{D}(\Omega).$$

Throughout this work we are mostly concerned with Sobolev spaces with $p = 2$. In this case, we set $H^k(\Omega) := W^{k,2}(\Omega)$ which is a Hilbert space for the inner product[3]

$$(u, v) := \sum_{|\alpha| \leq k} (D^\alpha u, D^\alpha v)_{L^2(\Omega)}.$$

One of the main tools used in the last section of this chapter is the following embedding theorem that relates the topologies of $H^1(\Omega)$ and $L^2(\Omega)$.

Theorem 2.3.6 (Rellich Theorem). *Assume that Ω is a bounded Lipschitz domain. Then, the embedding $H^1(\Omega) \to L^2(\Omega)$ is compact, i.e, given the bounded sequence $(u_n)_{n \in \mathbb{N}} \subset H^1(\Omega)$ there exists a convergent subsequence $(u_{n_k})_{k \in \mathbb{N}} \subset L^2(\Omega)$.*

While we have only defined Sobolev spaces for $k \in \mathbb{N}$, it is possible to define fractional Sobolev spaces with a real exponent $s \in \mathbb{R}_0^+$. In particular, such a generalization can be made using Fourier Transforms if $p = 2$. Below we give an equivalent definition for a function $u \in H^k(\mathbb{R}^d)$.

---

[3]Observe that if $k = 0$ then $H^0(\Omega) = L^2(\Omega)$

Lemma 2.3.7. *Let* $u \in L^2(\mathbb{R}^d)$. *Then*

$$u \in H^k(\mathbb{R}^d) \iff (1 + |\xi|^k)\hat{u} \in L^2(\mathbb{R}^d)$$

where $\hat{u} = \mathcal{F}u$ *denotes the Fourier Transform of* u, *given by* $\mathcal{F}u(\xi) = \hat{u}(\xi) = \int_{\mathbb{R}^d} e^{-2\pi x \xi} u(x) d\xi$.

The above characterization of the $H^k(\mathbb{R}^d)$ space motivate the following definition

Definition 2.3.8. *Let* $s \in \mathbb{R}$. *We define*

$$H^s(\mathbb{R}^d) = \{u \in L^2(\mathbb{R}^d) : (1 + |\xi|^2)^{\frac{s}{2}} \hat{u} \in L^2(\mathbb{R}^d)\}$$

with the norm

$$\|u\|_{H^s(\mathbb{R}^d)} = \|(1 + |\xi|^2)^{\frac{s}{2}} \hat{u}\|_{L^2(\mathbb{R}^2)}.$$

The definition above only holds for Sobolev spaces defined over the whole space $\mathbb{R}^d$. In this work we are mostly concerned with the behavior over a bounded set $\Omega \subset \mathbb{R}^d$. Unfortunately, there are multiple definitions of fractional Sobolev spaces over a bounded set that may not agree between themselves if the boundary of Ω is not smooth enough (if the boundary fails to be parameterized by a continuous function). In any case, the following definition suffices for this work, see [8], [9] or [10].

Definition 2.3.9. *Let* $\Omega \subset \mathbb{R}^d$ *be a bounded set with Lipschitz boundary. We define*

$$\mathring{H}^s(\Omega) = \{v \in H^d(\mathbb{R}^d) : \operatorname{supp} v \subset \overline{\Omega}\}$$

and

$$H^s(\Omega) = H^s(\mathbb{R}^d) \setminus \mathring{H}^s(\mathbb{R}^d \setminus \Omega).$$

The norm of a function $u \in H^s(\Omega)$ *is given by*

$$\|u\|_{H^s(\Omega)} = \inf\{\|\tilde{u}\|_{H^s(\mathbb{R}^d)} : \tilde{u} \in H^s(\mathbb{R}^d), \ \tilde{u}_{|\Omega} = u\}.$$

Fractional Sobolev spaces are important for our study because they are deeply related with the boundary behavior of a given function. For example, if $u \in H^1(\Omega)$ and Ω is bounded and a Lipschitz domain, then $u_{|\partial\Omega} \in H^{\frac{1}{2}}(\partial\Omega)$. However, the statement above must be defined rigorously: not only u is only defined in the open set Ω, but u is only defined *almost everywhere* and the Lebesgue measure of $\partial\Omega$ is zero. Intuitively, we consider the continuous extension of functions from Ω to the boundary $\partial\Omega$ which is only possible if domain is regular *enough*. This is done in context of trace theory, c.f [11] and [12].

Theorem 2.3.10. *Let Ω be a bounded set with Lipschitz boundary. Then, there exists a linear and continuous mapping called the trace operator*

$$\gamma_0 : H^1(\Omega) \to H^{\frac{1}{2}}(\partial\Omega)$$

that admits a bounded right inverse represented by γ_0^{-1}.

In particular, if $u \in H^2(\Omega)$, then $\frac{\partial u}{\partial x_j} \in H^1(\Omega)$ for $j = 1, \ldots, d$ and the operator

$$\gamma_1 : H^2(\Omega) \to L^2(\partial\Omega)$$
$$u \mapsto \frac{\partial u}{\partial n} = \gamma_0(\nabla u) \cdot n$$

is linear and continuous[4].

The result above is stated in a very weak form since we are working in Lipschitz domains. If Ω is a smooth domain, then $\gamma_1 : H^2(\Omega) \to H^{\frac{1}{2}}(\partial\Omega)$ (c.f [5]). However, it should be noted that the normal derivative operator γ_1 cannot be defined if we only assume that $u \in H^1(\Omega)$. If such a continuous operator $\mathcal{N}$ existed, then $\mathcal{N}\varphi = 0$ for every $\varphi \in \mathcal{D}(\Omega)$. By continuity, this would imply $\mathcal{N}u = 0$ for all $u \in H^1(\Omega)$, leading to a contradiction.

An important (closed) subspace of $H^1(\Omega)$ is the kernel of the trace operator γ_0,

$$\ker \gamma_0 = \{u \in H^1(\Omega) : \gamma_0 u = 0\} =: H_0^1(\Omega)$$

which can be equivalently defined as the closure of $\overline{\mathcal{D}(\Omega)}$ in the $H^1(\Omega)$ norm, i.e, $H_0^1(\Omega) := \overline{\mathcal{D}(\Omega)}^{H^1(\Omega)}$. $H_0^1(\Omega)$ is of major importance in the Dirichlet Laplacian problem, since the functions in $H_0^1(\Omega)$ "vanish" on $\partial\Omega$. Next, we state an important result to be used when studying the spectrum of the Dirichlet Laplacian.

Theorem 2.3.11 (Poincaré inequality)**.** *Let Ω be a bounded set. Define $W_0^{1,p}(\Omega) := \overline{\mathcal{D}(\Omega)}^{W^{1,p}(\Omega)}$. Then, there exists $C > 0$ such that*

$$\|u\|_{L^p(\Omega)} \leq C\|\nabla u\|_{L^p(\Omega)}, \ \forall u \in W^{1,p}(\Omega).$$

Finally, we shed some light over the dual space of Sobolev spaces (with fractional exponent). When working over the whole space $\mathbb{R}^d$ one can prove the following result, c.f [13] or [14].

Theorem 2.3.12. *Let $s \in \mathbb{R}$ and $u \in H^s(\mathbb{R}^d)$. Then, any linear and continuous functional $T \in (H^s(\mathbb{R}^d))^\star$ that acts in $H^s(\mathbb{R}^d)$ can be uniquely represented by some $v \in H^{-s}(\mathbb{R}^d)$ and the duality pairing is given*

---

[4]We take γ_0 as an element wise operator, where $\gamma_0(\nabla u) = \left(\gamma_0(\frac{\partial u}{\partial x_1}), \ldots, \gamma_0(\frac{\partial u}{\partial x_d})\right)$.

by

$$\langle T, u \rangle_{(H^s(\mathbb{R}^d))^\star, H^s(\mathbb{R}^d)} = \int_{\mathbb{R}^d} \hat{u}\hat{v} = \int_{\mathbb{R}^d} (1 + |\xi|^2)^{\frac{s}{2}} \hat{u}(1 + |\xi|^2)^{-\frac{s}{2}} \hat{v} \leq \|u\|_{H^s(\Omega)} \|v\|_{H^{-s}(\Omega)}$$

where $\hat{u}$ and $\hat{v}$ represents the Fourier Transform of u and v, respectively. In particular, the dual of $H^s(\mathbb{R}^d)$ is isomorphic to $H^{-s}(\mathbb{R}^d)$.

Remark 2.3.13. *Considering the inclusion $\mathcal{D}(\Omega) \subset H^s(\Omega)$, it is straightforward to observe that $(H^s(\Omega))^\star \subset D^\star(\Omega)$ which implies that $L^2(\Omega) \subset (H^s(\Omega))^\star \cong H^{-s}(\Omega)$. Consequently, based on the preceding theorem, we note that Sobolev spaces with negative exponent s can be regarded as spaces of distributions with the following inclusions:*

$$H^s(\Omega) \subset L^2(\Omega) \subset H^{-s}(\Omega)$$

In this case, one can consider $L^2(\Omega)$ as a pivot space, and by virtue of the identification of $L^2(\Omega)$ with its dual, the duality pairing $\langle \cdot, \cdot \rangle_{H^{-s}(\Omega), H^s(\Omega)}$ and the $L^2(\Omega)$ inner product coincide for every $u \in H^s(\Omega)$ and

$$\langle v, u \rangle_{H^{-s}(\Omega), H^s(\Omega)} = \int_\Omega uv$$

whenever it makes sense, i.e, when $v \in L^2(\Omega)$.

Theorem 2.3.10 allows to give some meaning to space $H^{-\frac{1}{2}}(\Omega)$. Let $u \in H^2(\Omega)$ and $v \in H^{\frac{1}{2}}(\partial\Omega)$. Then, $\gamma_0^{-1}v \in H^1(\Omega)$ and using Green's formula (see in the section below)

$$\langle \gamma_1 u, v \rangle_{H^{-\frac{1}{2}}(\partial\Omega), H^{\frac{1}{2}}(\partial\Omega)} = \int_\Omega \Delta u \gamma_0^{-1}v + \int_\Omega \nabla u \cdot \nabla \gamma_0^{-1}v$$

we have $\gamma_1 u \in H^{-\frac{1}{2}}(\Omega)$.

2.4 Spectral Decomposition of the Laplace Operator

In this section, we make a brief study regarding the Laplace Operator $-\Delta = -\sum_{n=1}^d \frac{\partial^2}{\partial x_n^2}$ in a bounded domain $\Omega \subset \mathbb{R}^d$ with Lipschitz boundary. Firstly, we recall the Divergence Theorem, e.g [15].

Theorem 2.4.1 (Divergence Theorem)**.** *Let $\Omega \subset \mathbb{R}^d$ defined as above. Then,*

$$\int_\Omega \operatorname{div} \phi dx = \int_{\partial\Omega} \phi \cdot \mathbf{n} d\sigma,$$

where $\mathbf{n}$ denotes the exterior unitary normal.

A main consequence of the Divergence Theorem are the well-known *Green's Formulas*, with major importance in this work.

Corollary 2.4.2 (Green's Formulas)**.** *In this same conditions of the Theorem 2.4, let $u, v \in H^2(U)$. Then,*

1. $\int_\Omega \Delta u dx = \int_{\partial\Omega} \frac{\partial u}{\partial n} d\sigma$;

2. $\int_\Omega \Delta u v dx = - \int_\Omega \nabla u \cdot \nabla v dx + \int_{\partial\Omega} \frac{\partial u}{\partial n} v d\sigma$;

3. $\int_\Omega \Delta u v - u \Delta v dx = \int_{\partial\Omega} \frac{\partial u}{\partial n} v - \frac{\partial v}{\partial n} u d\sigma$.

The study of the spectrum of the following equation is of major importance throughout this work, and will be studied in the following chapter. For now, we will only state and prove a classical result which can also be found in numerous textbooks, see [3] [4], [16] or [17]. While we assume null Dirichlet boundary conditions, we notice that the Neumann case is analogous.

Definition 2.4.3. *Consider the Helmholtz equation with null Dirichlet boundary conditions*

$$\begin{cases} -\Delta u(x) = \lambda u(x), & x \in \Omega, \\ u(x) = 0, & x \in \partial\Omega, \end{cases} \tag{2.1}$$

where $\Delta = \sum_{i=0}^d \frac{\partial^2}{\partial x_i^2}$. Then, $\lambda \in \mathbb{C}$ is an eigenvalue of the equation (2.1) *if there exists an eigenfunction $u \neq 0$ belonging to the function spaces $C^2(\Omega) \cap C(\overline{\Omega})$.*

Theorem 2.4.4. *There exists a Hilbert basis $(u_n)_{n\in\mathbb{N}}$ of $L^2(\Omega)$ consisting of eigenfunctions u_n of $-\Delta$, i.e, for each $n \in \mathbb{N}$ there exists a pair eigenvalue/eigenfunction (λ_n, u_n) such that*

$$-\Delta u_n = \lambda_n u_n$$

where the sequence of eigenvalues can be ordered in an increasing order and $\lambda_n \to \infty$, $n \to \infty$. In particular, define $E_n = \mathrm{span}\{u_1, \ldots, u_n\}$ and the Rayleigh Quotient

$$R(u) = \frac{\|\nabla u\|_{L^2(\Omega)}^2}{\|u\|_{L^2(\Omega)}^2}.$$

Then,

$$\lambda_n = \min_{\substack{u\in E_{n-1}^\perp \\ u\neq 0}} R(u) = \max_{\substack{u\in E_n \\ u\neq 0}} R(u).$$

Proof. For each $f \in L^2(\Omega)$, we consider the problem

$$\begin{cases} -\Delta u(x) = f, & \text{in } \Omega \\ u = 0, & \text{on } \partial\Omega \end{cases}$$

with the associated variational form

$$\int_\Omega \nabla u \cdot \nabla v = \int_\Omega fv, \ \forall v \in H_0^1(\Omega).$$

Using Lax-Milgram Theorem 2.2.7, it is straightforward to prove that the variational form above admits a unique weak solution $u \in H_0^1(\Omega)$ and the operator

$$T : L^2(\Omega) \to L^2(\Omega)$$
$$f \mapsto u$$

is well-defined. To prove that T is a compact operator, we use Poincaré and Cauchy-Schwarz inequalities and notice that

$$\alpha \|u\|_{H^1(\Omega)}^2 \leq \int_\Omega |\nabla u|^2 = \int_\Omega fu \leq \|f\|_{L^2(\Omega)} \|u\|_{L^2(\Omega)} \leq \|f\|_{L^2(\Omega)} \|u\|_{H^1(\Omega)} \implies \|u\|_{H^1(\Omega)} \leq C\|f\|_{L^2(\Omega)}$$

where $\alpha, C > 0$. The above result can be written as

$$\|Tf\|_{H^1(\Omega)} \leq C\|f\|_{L^2(\Omega)}, \ \forall f \in L^2(\Omega)$$

and by Theorem 2.3.6 T is a compact operator. To check that T is self-adjoint it suffices to consider the weak variational form of the null Dirichlet boundary problems

$$-\Delta u = f \qquad -\Delta v = g$$

for $f, g \in L^2(\Omega)$ and apply Green's formulas. It is also easy to see that $(Tf, f)_{L^2(\Omega)} \geq 0, \forall f \in L^2(\Omega)$ since

$$\int_\Omega (Tf)f = \int_\Omega uf = \|\nabla u\|_{L^2(\Omega)}^2 \geq 0.$$

Applying the Spectral Theorem 2.2.15 to T, there exists a Hilbert basis $(u_n)_{n \in \mathbb{N}}$ such that

$$Tu_n = \mu_n u_n$$

for $\mu_n \in \mathbb{R}$, $\mu_n \to 0$ as $n \to \infty$. In particular, taking $f = \lambda_n u_n$, where $\lambda_n = \frac{1}{\mu_n}$, one can write

$$-\Delta u_n = \lambda_n u_n,$$

or in the integral form

$$\int_\Omega |\nabla u|^2 = \lambda_n \int_\Omega u^2,$$

with $\lambda_1 \leq \lambda_2 \leq \cdots \to \infty$. To check the variational form of the eigenvalues λ_n, let $u \in E_{n-1}^\perp$. Then,

$$
\begin{aligned}
\|\nabla u\|_{L^2(\Omega)}^2 = (\nabla u, \nabla u)_{L^2(\Omega)}^2 &= \Big(\sum_{m \geq n} (u, u_m)_{L^2(\Omega)} \nabla u_m, \nabla u \Big)_{L^2(\Omega)} \\
&= \sum_{m \geq n} (u, u_m)_{L^2(\Omega)} (\nabla u_m, \nabla u)_{L^2(\Omega)} \\
&= \sum_{m \geq n} \lambda_m (u, u_m)_{L^2(\Omega)} (u_m, u)_{L^2(\Omega)} \\
&\geq \lambda_n \sum_{m \geq n} \big| (u, u_m)_{L^2(\Omega)} \big|^2 \\
&= \lambda_n \|u\|_{L^2(\Omega)}^2
\end{aligned}
$$

where we used the bilinearity of the inner product, the fact that the sequence λ_n is non-decreasing and the Parseval's identity. It is easy to check that the equality is only attained if and only if u is in the eigenspace of λ_k. This proves that

$$
\lambda_n = \min_{\substack{u \in E_{n-1}^\perp \\ u \neq 0}} R(u).
$$

The other case is analogous. $\qquad\square$

Remark 2.4.5. *Observe that* (2.4.4) *only guarantees that the eigenfunctions u_n belong to $H_0^1(\Omega)$. In order to achieve the regularity stated in Definition* (2.4.3)*, some conditions on Ω should be imposed: for example, if Ω is an open set of class C^2. If Ω is smooth, then $u_n \in C^\infty(\overline{\Omega})$.*

Corollary 2.4.6 (Homogeneity)**.** *Let $\alpha > 0$. Consider the set*

$$
\alpha\Omega = \{\alpha x \in \mathbb{R}^d : x \in \Omega\},
$$

i.e, $\alpha\Omega$ is a dilation of Ω by a factor of scale α. Then, for all $n \in \mathbb{N}$,

$$
\alpha^2 \lambda_n(\alpha\Omega) = \lambda(\Omega),
$$

where $\lambda_n(\alpha\Omega)$ is the n-esim eigenvalue of (2.1) *on the domain $\alpha\Omega$ (and analogously for $\lambda_n(\Omega)$).*

Proof. The proof is an easy consequence of the variational description above. Let $\varphi(x) = \alpha x$ and $\alpha\Omega = \phi(\Omega)$. Then,

$$
\lambda_n(\alpha\Omega) = \min_{\substack{u \in E_{n-1}^\perp \\ u \neq 0}} \frac{\int_{\varphi(\Omega)} |\nabla u(x)|^2 dx}{\int_{\varphi(\Omega)} u(x)^2 dx} = \min_{\substack{u \in E_{n-1}^\perp \\ u \neq 0}} \frac{\int_\Omega |\nabla u(\alpha x)|^2 dx}{\int_\Omega u(\alpha x)^2 dx},
$$

via a change of variables. Let $v(x) = u(\alpha x)$. Then,

$$\nabla v(x) = \alpha \nabla u(\alpha x)$$

and

$$\alpha^2 \lambda_n(\alpha \Omega) = \min_{\substack{u \in E_{n-1}^{\perp} \\ u \neq 0}} \frac{\int_{\Omega} |\alpha \nabla u(\alpha x)|^2 dx}{\int_{\Omega} u(\alpha x)^2 dx} = \min_{\substack{u \in E_{n-1}^{\perp} \\ u \neq 0}} \frac{\int_{\Omega} |\nabla v(x)|^2 dx}{\int_{\Omega} v(x)^2 dx} = \lambda_n(\Omega).$$

$\square$

3

From Spectral Theory and Shape Optimization to the Poisson Transmission Problem

Contents

Until otherwise indicated, let $\Omega \subset \mathbb{R}^d$ be an open and bounded domain with C^2 boundary, with $d \geq 2$.

Let $p(x)$ be a polynomial in the variables $x = (x_1, \ldots, x_d)$, and $p(\partial)$ be the partial differential operator obtained by substituting $\frac{\partial}{\partial x_i}$ for x_i in $p(x)$. We start by introducing the definition of a fundamental solution of a partial differential operator:

Definition 3.0.1. *Consider the polynomial $p(\partial)$. A distribution $\Phi \in \mathcal{D}^\star(\mathbb{R}^n)$ is said to be the fundamental solution of the partial differential operator $p(\partial)$ if*

$$p(\partial)\Phi = \delta,$$

where δ is the Dirac Delta distribution.

In particular, given Φ satisfying the above conditions, we have that $p(\partial)\Phi(x) = 0$ for $x \in \mathbb{R}^d \setminus \{0\}$. Then, it is easy to see that the fundamental solution of a partial differential operator is not unique: if Φ is such that $p(\partial)\Phi = \delta$ and $p(\partial)v(x) = 0$ for all $x \in \mathbb{R}^d$, then $p(\partial)(\Phi + v) = \delta$. However, the fundamental solutions given below are chosen because they exhibit an important radial behavior, which is needed for the numerical method presented in Chapter 4.

An important result in this context is Malgrange-Ehrenpreis theorem.

Theorem 3.0.2 (Malgrange-Ehrenpreis)**.** *Every constant partial differential operator $p(\partial)$, has a fundamental solution $\Phi \in \mathcal{D}^\star(\mathbb{R}^d)$.*

Proof. See [18]. $\qquad\qquad\qquad\qquad\qquad\qquad\qquad\qquad\qquad\qquad\qquad\qquad\qquad\qquad\square$

Below we present the fundamental solution of Laplace differential operator and some major results concerning Laplace and Helmholtz equations.

3.1 The Laplace Operator

In what follows, we present some results of the Laplace operator associated with the well-known Laplace equation

$$-\Delta u = 0. \tag{3.1}$$

Throughout this first part we are mostly concerned about its spectrum which is associated with the Helmholtz equation

$$-(\Delta + \lambda)u = 0 \iff -\Delta u = \lambda u. \tag{3.2}$$

Remark 3.1.1. *In some literature, it is common to write the Helmholtz equation as $-\Delta u = k^2 u$, where k is known as an eigenfrequency, and $k^2 = \lambda$. This terminology is a consequence of the fact that the Helmholtz equation can be derived from the wave equation, where a constant c^2 (where $c \in \mathbb{R}$) is used.*

By Theorem 3.0.2 we know that both equations (3.1) and (3.2) admit a fundamental solution that are given below.

Proposition 3.1.2. *The function $\Phi : \mathbb{R}^d \setminus \{0\} \to \mathbb{R}$ given by*

$$\Phi(x) = \begin{cases} -\frac{1}{2\pi} \log |x|, & d = 2 \\ \frac{1}{(n-2)|\partial B_1|} \frac{1}{|x|^{d-2}}, & d > 2 \end{cases}$$

is the fundamental solution of equation (3.1), where $|\partial B_1|$ denotes the boundary measure of the unitary ball.

Proposition 3.1.3. *The function $\Phi_\lambda : \mathbb{R}^d \setminus \{0\} \to \mathbb{R}$ given by*

$$\Phi_\lambda(x) = \begin{cases} \frac{i}{4} H_0^{(1)}(\sqrt{\lambda}\|x\|), & d = 2 \\ \frac{e^{i\sqrt{\lambda}\|x\|}}{4\pi\|x\|}, & d > 2 \end{cases}$$

is the fundamental solution of equation (3.2), where $H_0^{(1)}$ is the Hankel function of first kind and order 0, given by

$$H_0^{(1)}(x) = J_0(x) + iY_0(x),$$

where J_0 and Y_0 are the Bessel functions of first and second kind with order zero, respectively.

If one considers the eigenfrequency form of the Helmholtz equation, then the fundamental solution in Proposition (3.1.3) would change accordingly.

3.1.1 Some shape optimization results

In this subsection some important results regarding shape optimization are presented. More precisely, we are interested in problems of the form

$$\min\{F(\lambda_1(\Omega), \dots, \lambda_k(\Omega)) : |\Omega| = c, \Omega \subset \mathbb{R}^d\}, \tag{3.3}$$

where F is a function of the first k eigenvalues of the Helmholtz equation (3.2) and $c > 0$. We point the reader to [19] and [20] to more details.

Theorem 3.1.4 (Faber-Krahn inequality). *Let B be a ball of volume c. Then, among all domains Ω of volume c we have that,*

$$\lambda_1(B) = \min\{\lambda_1(\Omega) : |\Omega| = c\}.$$

In particular, as proved by Krahn in [21], the corresponding isoperimetric inequality

$$\lambda_1(\Omega) \geq \left(\frac{C_d}{c}\right)^{\frac{d}{2}} j_{d/2-1,1},$$

where C_d is the volume of the d-dimensional unit ball and $j_{p,1}$ is the first positive zero of the Bessel function J_p, holds.

Theorem (3.1.4) is a classic form of an isoperimetric inequality, conjectured for the first time by Lord Rayleigh. More recently, a reverse of the Faber-Krahn inequality was proven in [22].

Theorem 3.1.5. *Let Ω be a bounded convex domain of $\mathbb{R}^d$ and denote the inradius of Ω (radius of the largest ball contained within the domain) by ρ_Ω. Then,*

$$\lambda_1(\Omega) \leq \frac{|\partial\Omega|}{d\rho_\Omega|\Omega|}\lambda_1(\mathbb{D})$$

While Faber-Krahn inequality deals with the first eigenvalue of the Laplace operator, other results have been uncovered for the second and third eigenvalues:

Theorem 3.1.6 (Krahn-Szegő)**.** *The domain that minimizes the quantity*

$$\min\{\lambda_2(\Omega) : |\Omega| = c\}$$

consists of two equal and disjoint balls of volume $\frac{c}{2}$.

A result regarding the topology of a given domain Ω and its connection with the minimization of each eigenvalue λ_k was given by Wolf and Keller in [23]. Roughly speaking, the result states that if a minimizer of λ_k is not connected, then each connected component must be a minimizer for a lower eigenvalue.

Theorem 3.1.7 (Wolf-Keller)**.** *Let $\Omega_k^\star$ be the union of two disjoint domains, each of them with positive volume. Then,*

$$\lambda_k^\star = (\lambda_i^\star)^{\frac{d}{2}} + (\lambda_{k-i}^\star)^{\frac{d}{2}} = \min_{1 \leq j \leq \frac{k-1}{2}}((\lambda_j^\star)^{\frac{d}{2}} + (\lambda_{k-j}^\star)^{\frac{d}{2}}),$$

where i is a value of $j \leq \frac{k-1}{2}$ that minimizes $\lambda_i^\star + \lambda_{k-i}^\star$. Furthermore,

$$\Omega_k^\star = \left[\left(\frac{\lambda_i^\star}{\lambda_k^\star}\right)^{\frac{1}{2}}\Omega_i^\star \bigcup \left(\frac{\lambda_{k-i}^\star}{\lambda_k^\star}\right)^{\frac{1}{2}}\Omega_{k-i}^\star\right]$$

The generalization of the Theorems (3.1.4) and (3.1.6) becomes harder to prove for high order eigenvalues. Bucur and Henrot proved in [24] that there exists a domain Ω that minimizes λ_3, and it is conjectured to be the disk[1]. In [25], Bucur was able to assert the existence of, at least, one solution to problem

---

[1]Notice that Ω_3 must be connected in dimension 2. Otherwise, by Theorem (3.1.7), Ω_3 would be the union of the domains that

(3.3).

Theorem 3.1.8 (Bucur)**.** *For every $k \in \mathbb{N}$ problem*

$$\min\{\lambda_k(\Omega) : |\Omega| = c\}$$

has at least one solution. Moreover, every solution is bounded and has finite perimeter.

In [26], Mazzoleni and Pratelli were able to generalize the above results for (*quasi-*)open sets and for a general functional F considered in (3.3) (see the reference for more details and definition of a quasi-open set).

Theorem 3.1.9 (Mazzoleni-Pratelli)**.** *Let $k \in \mathbb{N}$ and suppose that $F : \mathbb{R}^k \to \mathbb{R}$ in (3.3) is lower semicontinuous, increasing in each variable. Then, among the quasi-open sets, there exists a bounded minimizer Ω for the problem (3.3). More precisely, a minimizer Ω is contained in a cube of side R, where R depends on k and on the dimension of the space d, but not on F.*

In this work, we are also interested in studying the eigenvalues of polygonal domains, such as triangles and quadrilaterals. An important result concerning these domains is the fact that they are invariant under the so-called *Steiner symmetrization* (in the sense that the Steiner symmetrization of a triangle or a quadrilateral is still a triangle or a quadrilateral, respectively), which preserves their area while decreasing the perimeter and its first eigenvalue. This type of transformation enables us to state the following result:

Theorem 3.1.10 (Pólya-Szégő)**.** *The quantity λ_1 is minimized for equilateral triangles among all triangles, where the inequality*

$$\frac{4\pi^2}{\sqrt{3}} \le \lambda_1(T)$$

holds for every triangle T of area 1. Analogously, λ_1 is minimized for the square among all quadrilaterals.

However, an analogous result for the n-side polygon is still an open problem conjectured by Pólya and Szégő in [27].

Conjecture 3.1.11. *Let $n \ge 5$ and consider the class of n-side polygons. Then, the regular n-side polygon has the least first eigenvalue among all n-side polygons with fixed area.*

Very recently, Bogosel and Bucur proved in [28] that Conjecture (3.1.11) can be reduced to a finite number of certified numerical computations with machine precision, and performed them for $k = 5, 6, 7, 8$.

Related to triangles, we can also cite the recent work of Serrano and Orriols in [29], which was based on the previous work of Antunes and Freitas [30] who conjectured that the first three eigenvalues are

---

minimize λ_1 and λ_2 (see Theorems (3.1.4) and (3.1.6)), where one can explicitly compute $\lambda_3 = \lambda_1 + \lambda_2 \approx 51.504$. However, this would be a contradiction since the eigenvalue of the unit disk is $\lambda_3(\mathbb{D}) \approx 46.125$, when considering unitary measure $c = 1$. For three dimensions the result is the same, but for $d \ge 4$ one cannot conclude anything.

enough to define the shape of a triangle (such result resembles the famous Marc Kac question if one can "hear the shape of a drum" in [31], that is, if given the frequencies produced by a drum one could identify the drum's shape, which has proven to be false, see [32] for more details). In any case, Serano and Orriols were able to show that not any three eigenvalues suffice to fully characterize the shape of a triangle.

Theorem 3.1.12 (Serrano-Orriols)**.** *There exist two triangles T_A and T_B not isometric to each other such that $\lambda_i(T_A) = \lambda_i(T_B)$, for $i = 1, 2, 4$.*

Other important results in this area are related with the ratio and the gap between the first and the second eigenvalues.

Theorem 3.1.13 (Ashbaugh-Benguria)**.** *The solution of the maximization problem*

$$\max\left\{\frac{\lambda_2(\Omega)}{\lambda_1(\Omega)} : \Omega \subset \mathbb{R}^d, \Omega \text{ open}\right\}$$

is the ball. In particular, it can be shown that

$$\frac{\lambda_2(\Omega)}{\lambda_1(\Omega)} \leq \frac{j_{\frac{d}{2},1}^2}{j_{\frac{d}{2}-1,1}^2}.$$

Remark 3.1.14. *Note that in theorem above we do not make any constraint regarding the volume of our domain (except finite measure). This as consequence of the homogeneity proven in Corollary* (2.4.6) *and the fact that we are now considering a ratio between two eigenvalues in the same domain.*

3.2 The Dirac Operator

Motivated by recent advancements in nuclear, molecular physics and the discovery of very interesting electrical, mechanical and thermal properties, Dirac materials have resurged a lot of attention in the Dirac equation. Presented by Paul Dirac in its 1928 article [33], Dirac equation was able to successfully merge the famous Schrödinger equation with special relativity, while explaining the weird phenomena that today is known as *spin*, while predicting the existence *antimatter*. Capable of describe the relativistic dynamics of spin-$\frac{1}{2}$ particles (like the electron), one can determine the energy states by studying the spectrum of the Hamiltonian (Dirac) operator $\hat{H}$ in $L^2(\Omega, \mathbb{C}^2)$ for $\Omega \subset \mathbb{R}^2$,

$$\hat{H}u = Eu \quad \text{with} \quad \hat{H} = c\,\mathbf{a} \cdot \mathbf{p} + mc^2\beta + V(x)\mathbb{I}_4, \tag{3.4}$$

where $\mathbf{p} = -i\nabla$ is the momentum operator, c is the speed of light, m is the electron mass, E is the electron energy, $V(x)$ is the vector potential and $u \in L^2(\Omega, \mathbb{C}^2)$ is a four-spinor[2]. One of the major problems regarding the study of Dirac's equation is the fact that, unlike Schrödinger's equation, it has a matrix structure that is given by the Pauli matrices

$$\sigma_x = \begin{bmatrix} 0 & 1 \\ 1 & 0 \end{bmatrix} \qquad \sigma_y = \begin{bmatrix} 0 & -i \\ i & 0 \end{bmatrix} \qquad \sigma_z = \begin{bmatrix} 1 & 0 \\ 0 & -1 \end{bmatrix}$$

which can be incorporated in the 4×4 matrices $\mathbf{a}$ and β:

$$a_i = \begin{bmatrix} 0 & \sigma_i \\ \sigma_i & 0 \end{bmatrix} \qquad \beta = \begin{bmatrix} \mathbb{I}_2 & 0 \\ 0 & -\mathbb{I}_2 \end{bmatrix}.$$

Setting the potential $V(x) = 0$ and considering $\Omega \subset \mathbb{R}^2$ be a bounded and open domain with C^3 boundary, we can rewrite equation (3.4) in the form

$$\begin{bmatrix} m & -i(\partial_1 - i\partial_2) \\ -i(\partial_1 + i\partial_2) & -m \end{bmatrix} \begin{bmatrix} u_1(x) \\ u_2(x) \end{bmatrix} = E \begin{bmatrix} u_1(x) \\ u_2(x) \end{bmatrix} \tag{3.5}$$

where we let $\mathbf{u}(x) = \begin{bmatrix} u_1(x) \\ u_2(x) \end{bmatrix}$. In particular, we are interested in studying it under the so-called *infinite-mass boundary conditions*. For a point $x \in \Gamma = \partial\Omega$, we denote by $\mathbf{n}(x) = \big(n_1(x), n_2(x)\big)^T$ the outward unit vector to Ω, and define the operator domain

$$D(\hat{H}) = \{u \in H^1(\Omega, \mathbb{C}^2) : u_2 = i(n_1 + in_2)u_1 \text{ on } \Gamma\}.$$

Let $\tau(x) = \big(n_2(x), -n_1(x)\big)^T$ be the unit tangent vector to some point $x \in \Gamma$ such that $(\tau(x), \mathbf{n}(x))$ is a positively-oriented orthonormal basis of $\mathbb{R}^2$. Considering the arc-length parametrization of Γ given by the map

$$s : [0, L] \to \mathbb{R}^2, \quad s(t) = \int_0^t \|r'(\sigma)\| d\sigma$$

where L represents the arc-length of Γ and r is a parametrization of Γ, we denote by $\kappa : \Gamma \to \mathbb{R}$ the signed curvature of Γ where the *Frenet-Serret* formula (we dropped the dependency of s in the parameter t)

$$\frac{\partial\tau}{\partial s} = \kappa(s)\mathbf{n}(s)$$

holds. Similar to the Theorem (2.4.4), some general results regarding the spectrum of the Dirac operator can also be stated.

Proposition 3.2.1. *Consider the eigenvalue problem stated in* (3.5)*. Then, the following results hold,* [3]

---

[2]In what follows, we will be using natural units, where $c = 1$.

[3]Notice that we changed the eigenvalue notation E to λ. Not only for coherence reasons, but also because we are mainly interested in the mathematical description of the problem, and not in the physical intuition behind it (the energy of a spin-$\frac{1}{2}$

- *The eigenvalues are real and the spectrum of the Dirac operator is discrete. Also, the spectrum is symmetric with respect to zero and the eigenvalues can be arranged as follows*

$$-\infty \leftarrow \cdots \leq -\lambda_3 \leq -\lambda_2 \leq -\lambda_1 < 0 < \lambda_1 \leq \lambda_2 \leq \lambda_3 \leq \cdots \rightarrow \infty;$$

- *The principal (first) eigenvalue can be described using the variational form*

$$\lambda_1^2 = \min_{0 \neq u \in D(\hat{H})} \frac{\|\nabla u\|_{L^2(\Omega)}^2 + m^2 \|u\|_{L^2(\Omega)}^2 + m\|\gamma_0 u\|_{L^2(\partial\Omega)}^2}{\|u\|_{L^2(\Omega)}^2},$$

where $\gamma_0 : H^1(\Omega, \mathbb{C}^2) \to L^2(\Gamma, \mathbb{C}^2)$ denotes the trace of u;

- *Let $m = 0$ and Ω to be the unit disk $\mathbb{D}$. Then, we have that the first eigenvalue is the solution to the equation*

$$J_0(\lambda) = J_1(\lambda),$$

and the associated eigenfunction is (in polar coordinates)

$$u(r, \theta) = \begin{pmatrix} J_0(\lambda r) \\ i e^{i\theta} J_1(\lambda r) \end{pmatrix}.$$

For future comparison, its numerical approximation is $\lambda \approx 1.434696$, where we recall that J_p is the Bessel function of first kind of order p.

The following proposition regarding the lack of separable solutions of the Dirac operator will have important consequences in the numerical approach to solve Dirac equation. However, we start by stating and proving the following auxiliary lemma:

Lemma 3.2.2. *Let $u \in H^2(\Omega)$ a solution of* (3.5) *and $u \in D(\hat{H})$. Then we have*

$$\|\hat{H}u\|_{L^2(\Omega)}^2 = \|\nabla u\|_{L^2(\Omega)}^2 + m^2 \|u\|_{L^2(\Omega)}^2 + m\|\gamma u\|_{L^2(\partial\Omega)}^2 - \frac{1}{2} \int_\Gamma \kappa |u|^2 d\sigma \tag{3.6}$$

Proof. Recalling the $L^2(\Omega)$ inner product for complex functions

$$(f, g)_{L^2(\Omega)} = \int_\Omega f\bar{g}dx,$$

---

particle).

(3.6) can be rewritten as

$$\|\hat{H}u\|_{L^2(\Omega)}^2 = m^2\|u_1\|_{L^2(\Omega)} + m^2\|u_2\|_{L^2(\Omega)} \tag{3.7}$$

$$+ im\int_\Omega u_1(\partial_1 + i\partial_2)\bar{u}_2 dx - im\int_\Omega \bar{u}_1(\partial_1 - i\partial_2)u_2 dx \tag{3.8}$$

$$+ im\int_\Omega \bar{u}_2(\partial_1 + i\partial_2)u_1 dx - im\int_\Omega u_2(\partial_1 - i\partial_2)\bar{u}_1 dx \tag{3.9}$$

$$+ \|(\partial_1 - i\partial_2)u_2\|_{L^2(\Omega)}^2 + \|(\partial_1 + i\partial_1)u_1\|_{L^2(\Omega)}^2. \tag{3.10}$$

We now address each line of the expression above individually:

- For (3.7) we directly have

$$m^2\|u\|_{L^2(\Omega)}.$$

- For (3.8) we integrate by parts the first part:

$$\int_\Omega u_1(\partial_1 + i\partial_2)\bar{u}_2 dx = \int_{\partial\Omega} u_1\bar{u}_2(1 + i)d\sigma - \int_\Omega \bar{u}_2(\partial_1 + i\partial_2)u_1 dx$$

where the last part cancels with the first part of (3.9).

- Analogously, for (3.9) we obtain a similar result for the last part

$$\int_\Omega u_2(\partial_1 - i\partial_2)\bar{u}_1 dx = \int_{\partial\Omega} u_2\bar{u}_1(1 - i)d\sigma - \int_\Omega \bar{u}_1(\partial_1 - i\partial_2)u_2 dx$$

where the last part cancels with the last part of (3.8).

- For (3.10) we firstly deduced the following property:

$$\mathrm{Im}\left(\int_\Omega \partial_1 v \partial_2 \bar{v} dx\right) = \frac{1}{2i}\int_{\partial\Omega} \bar{v}\partial_\tau v d\sigma, \ \forall v \in H^2(\Omega),$$

where $\partial_\tau v = \tau \cdot \nabla v$, which can be obtained using integration by parts. Then, for each part we have

$$\|(\partial_1 - i\partial_2)u_2\|_{L^2(\Omega)}^2 = \|\nabla u_2\|_{L^2(\Omega)}^2 + i\left(\int_\Omega \partial_1 u_2 \partial_2 \bar{u}_2 dx - \int_\Omega \partial_2 u_2 \partial_1 \bar{u}_2 dx\right)$$

$$= \|\nabla u_2\|_{L^2(\Omega)}^2 + i\int_{\partial\Omega} \bar{u}_2 \partial_\tau u_2 d\sigma$$

$$\|(\partial_1 + i\partial_2)u_1\|_{L^2(\Omega)}^2 = \|\nabla u_1\|_{L^2(\Omega)}^2 - i\left(\int_\Omega \partial_1 u_1 \partial_2 \bar{u}_1 dx - \int_\Omega \partial_2 u_1 \partial_1 \bar{u}_1 dx\right)$$

$$= \|\nabla u_1\|_{L^2(\Omega)}^2 - i\int_{\partial\Omega} \bar{u}_1 \partial_\tau u_1 d\sigma$$

where we used the property above.

As such, we can write everything as

$$\|\hat{H}u\|^2_{L^2(\Omega)} = m^2\|u\|_{L^2(\Omega)} + im\Big(\int_{\partial\Omega} u_1\bar{u}_2(1+i)d\sigma - \int_{\partial\Omega} u_2\bar{u}_1(1-i)d\sigma\Big)$$
$$+ \|\nabla u\|_{L^2(\Omega)} + i\Big(\int_{\partial\Omega} \bar{u}_2\partial_\tau u_2 d\sigma - \int_{\partial\Omega} \bar{u}_1\partial_\tau u_1 d\sigma\Big).$$

Finally, using the boundary conditions $u_2 = i(n_1 + in_2)u_1$, we conclude that

$$im\Big(\int_{\partial\Omega} u_1\bar{u}_2(1+i)d\sigma - \int_{\partial\Omega} u_2\bar{u}_1(1-i)d\sigma\Big) = \|\gamma u\|^2_{L^2(\partial\Omega)}$$

while

$$i\int_{\partial\Omega} \bar{u}_2\partial_\tau u_2 d\sigma - i\int_{\partial\Omega} \bar{u}_1\partial_\tau u_1 d\sigma = -\frac{1}{2}\int_{\partial\Omega} \kappa|u|^2 d\sigma$$

where we used the Frenet-Serret formula above and the fact that at $\partial\Omega$ we have $|u_1|^2 = |u_2|^2$.   □

Proposition 3.2.3. *Let $u \in H^2(\Omega)$ a solution of* (3.5) *and $u \in D(\hat{H})$. Then u cannot be written using separable solutions.*

Proof. We start by showing that $|\lambda| > m$ for any eigenvalue λ if $\kappa = 0$ a.e. Assuming that there exists an eigenvalue λ associated with an eigenfunction u such that $|\lambda| \leq m$, by using Lemma 3.2.2 we get that

$$\|\nabla u\|^2_{L^2(\Omega)} + m\|\gamma u\|^2_{L^2(\partial\Omega)} \leq 0 \implies \|\nabla u\|_{L^2(\Omega)} = 0 \wedge m\|\gamma u\|_{L^2(\partial\Omega)} = 0$$

and u must be a constant, which does not satisfy the boundary conditions.

Since $u \in H^2(\Omega)$, using (3.5), we can express u_2 as

$$u_2 = \frac{-i(\partial_1 + i\partial_2)u_1}{\lambda + m}$$

allowing us to rewrite Dirac equation (3.5) using the Helmholtz equation with Cauchy–Riemann oblique boundary conditions:

$$\begin{cases} -\Delta u_1 = (\lambda^2 - m^2)u_1, & \text{in } \Omega \\ i(\partial_1 + i\partial_2)u_1 + (\lambda + m)i(n_1 + in_2)u_1 = 0, & \text{on } \Omega. \end{cases} \tag{3.11}$$

The rest of the proof will have in consideration two domain types: triangular (on a wedge) and rectangular.

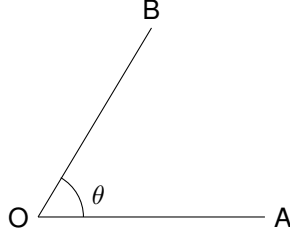1. Consider Ω to be a wedge domain with angle θ (see Figure 4.1):

Figure 3.1: A wedge domain with an interior angle θ.

In this case, since the outward unit normal on $\overline{OA}$ is $n = \begin{pmatrix} 0 \\ -1 \end{pmatrix}$ and on $\overline{OB}$ is $n = \begin{pmatrix} -\sin\theta \\ \cos\theta \end{pmatrix}$, using polar coordinates system (3.11) transforms into

$$
\begin{cases}
\left(\partial_r^2 + \frac{1}{r}\partial_r + \frac{1}{r^2}\partial_\theta^2\right)u_1 = (\lambda^2 - m^2)u_1, & \text{in } \Omega \\
i(\cos\theta\partial_r - \frac{1}{r}\sin\theta\partial_\theta + i(\sin\theta\partial_r + \frac{1}{r}\cos\theta\partial_\theta))u_1 + (\lambda + m)u_1 = 0, & \text{on } \overline{OA} \\
i(\cos\theta\partial_r - \frac{1}{r}\sin\theta\partial_\theta + i(\sin\theta\partial_r + \frac{1}{r}\cos\theta\partial_\theta))u_1 + (\lambda + m)i(-\sin\theta + i\cos\theta)u_1 = 0, & \text{on } \overline{OB}
\end{cases}
$$
$$(3.12)$$

As such, assuming that exists a solution $u_1(r,\theta) = \phi(r)T(\theta)$ of the system (3.12), from the boundary condition of $\overline{OB}$ one finds the equation

$$
\frac{e^{i\theta}\left(\phi(r)T'(\theta) + rT(\theta)\left((\lambda+m)\phi(r) - i\phi'(r)\right)\right)}{r} = 0
$$

which can be rewritten as

$$
\frac{T(\theta)}{T'(\theta)} = -\frac{\phi(r)}{r\left(m\phi(r) + \lambda\phi(r) - i\phi'(r)\right)} = -k^2
$$

for some $k \in \mathbb{R}$. Solving the equations above we find that

$$
u_1(r,\theta) = Ae^{-\frac{\theta}{k^2}}r^{\frac{i}{k^2}}e^{-ir(\lambda+m)}, \ A \in \mathbb{R}\setminus\{0\}.
$$

Substituting in the boundary condition for $\overline{OA}$ we obtain

$$
A\left(1 + e^{i\theta}\right)r^{\frac{i}{k^2}}(\lambda + m)e^{-\frac{\theta}{k^2} - ir(\lambda+m)} = 0
$$

where we conclude that $\lambda = -m$ (since if $\theta = \pi$ we would have a degenerate wedge), a contradiction.

2. For rectangular domains, we point the proof in [34].

$\square$

Remark 3.2.4. *A careful reader will note that two important details are being overlooked: triangular domains or quadrilaterals do not have the required smoothness to obtain the formula* (3.6) *(and signed curvature is not defined everywhere, only on each edge where $\kappa = 0$), neither u has enough regularity to be integrated by parts while expanding* (3.10). *We point to [35], where such details can be found for triangles, but are analogous for quadrilaterals.*

We now present some open conjectures that we try numerically address in this work:

Conjecture 3.2.5 (A Faber-Krahn type inequality)**.** *Let $m \geq 0$ and $\Omega \subset \mathbb{R}^2$ an open and Lipschitz domain. Then,*

$$\lambda_1(\Omega) \geq \lambda_1(\Omega^*)$$

where Ω^* is the disk of the same area or perimeter as Ω.

Conjecture above is regarded as a hot open problem in spectral geometry [36]. In [37] a geometric lower bound for the first (non-negative) eigenvalue was found, while in [38] a sharp upper bound (a reverse Faber-Krahn type inequality, like in Theorem 3.1.5) was proved to hold for convex domains with C^3 boundary. However, due to the difficulty of the problem, simpler versions with domain restrictions to triangles and rectangles are being studied. For example, in [34] a study for rectangles was conducted, where the conjectures below were proved under some extra hypothesis:

Conjecture 3.2.6 (Shape optimization in rectangles)**.** *Given $m \geq 0$, let $\lambda_1(a, b) = \lambda_1(\Omega_{a,b})$ denote the first eigenvalue of the Dirac Operator with infinite-mass boundary conditions in a rectangle with sides a and b. Then,*

1. *Area constraint: $\lambda_1(a, \frac{1}{a}) \geq \lambda_1(1, 1)$, $\forall a > 0$;*

2. *Perimeter constraint: $\lambda_1(a, 2 - a) \geq \lambda_1(1, 1)$, $\forall a \in (0, 2)$.*

In the same vain, in [35] very similar results were proven for triangles:

Conjecture 3.2.7 (Shape optimization in triangles)**.** *Consider the triangle $\Omega_{a,b}$ defined by the points $O = (0, 0), A = (a, 0), B = (0, b)$ for $a, b > 0$. Then, given any $m \geq 0$,*

1. *Area constraint: $\lambda_1(a, b) \geq \lambda(k, k)$, $\forall a, b, k > 0$ such that $ab = k^2$;*

2. *Perimeter constraint: $\lambda_1(a, b) \geq \lambda(k, k)$, $\forall a \in (0, (2 + \sqrt(2)k))$ and $\forall b, k > 0$ such that $a + b + \sqrt{a^2 + b^2} = (2 + \sqrt{2})k$.*

3.3   A domain decomposition problem

We now consider the polygonal domain $\Omega \subset \mathbb{R}^2$ which we divide into two non-overlapping regions Ω_1 and Ω_2 such that $\overline{\Omega} = \overline{\Omega_1} \cup \overline{\Omega_2}$. We denote their common boundary by $\gamma = \partial\Omega_1 \cap \partial\Omega_2$ and denote by

$\Gamma_i = \partial\Omega_1 \setminus \gamma$ the boundary of each domain Ω_1 minus the common boundary. The problem we address this section is to find functions u_1, u_2 such that

$$-\nabla k_i \nabla u_i = f_i, \text{ in } \Omega_i$$
$$u_1 - u_2 = 0, \text{ on } \gamma$$
$$k_1 \frac{\partial u_1}{\partial n_1} + k_2 \frac{\partial u_2}{\partial n_2} = 0, \text{ on } \gamma \tag{3.13}$$
$$u_i = 0, \text{ on } \Gamma_i$$

where $k_1 \geq k_2 > 0$ are constants, $f_i \in L^2(\Omega_i)$ is a source function on each domain and n_i is the (normalized) outward normal to each domain subdomain $\Omega_i, i = 1, 2$. Finally, we will write $n = n_1 = -n_2$ when we are restricted to the interface.

In what follows we mainly used the reference [39]. Equations (3.13) can be used to study a system of two bodies with different material parameters (contact resistance or thermal conductivity) connected by an interface γ. If we set

$$f = \begin{cases} \frac{f_1}{k_1}, & \Omega_1 \\ \frac{f_2}{k_2}, & \Omega_2 \end{cases},$$

then the problem above can be seen as a natural reformulation of the Poisson equation

$$-\Delta u = f, \text{ in } \Omega$$
$$u = 0, \text{ on } \partial\Omega \tag{3.14}$$

where f is (possibly) discontinuous on the interface γ. In order to keep the equivalence between both problems, we enforce some transmission conditions in Equations (3.13) using the continuity of the solutions and the continuity of their normal derivative on γ. To establish the equivalence between both problems we write the variational weak form associated with them. For (3.14) it's an easy process: we multiply the equation in Ω by a test function $v \in C_0^\infty(\Omega)$ and using Green's Identity we find that

$$a(u, v) = \int_\Omega \nabla u \cdot \nabla v = \int_\Omega fv$$

where a is the associated bilinear form. As such, enlarging our functional space to the Hilbert Space $V^0 = H_0^1(\Omega)$, our problem can be rewritten as

$$\text{find } u \in V^0 : a(u, v) = (f, v), \ \forall v \in V^0 \tag{3.15}$$

which has a unique solution in V^0 by virtue of Lax-Milgram lemma. In fact, by regularity results (see Section 6.3.1 of [7]), we're looking for $u \in V^0 \cap H_{\text{loc}}^2(\Omega'), \ \forall \Omega' \Subset \Omega^4$.

For (3.13) the process is not so direct. For the first equation, for the subdomain Ω_1, we multiply it

---

[4]We say that $A \Subset B$ when $\overline{A}$ is compact and $\overline{A} \subset B$.

with a test function in $v_1 \in C_0^\infty(\Omega_1)$ and integrate by parts where we get

$$a(u_1, v_1) = \int_{\Omega_1} \nabla u_1 \cdot \nabla v_1 = \left(\frac{f_1}{k_1}, v_1\right)$$

and analogously, for the subdomain Ω_2, considering $v_2 \in C_0^\infty(\Omega_2)$ we find

$$a(u_2, v_2) = \int_{\Omega_2} \nabla u_2 \cdot \nabla v_2 = \left(\frac{f_2}{k_2}, v_2\right).$$

To add the interface condition on the normal derivative we notice that if we take $v \in C_0^\infty(\Omega)$, we can define $v_1 = v_{\Omega_1}$ and $v_2 = v_{\Omega_2}$, where $v_i \in C^\infty(\Omega_i)$ and $v_i(x) = 0, \ \forall x \in \Gamma_i$ for $i = 1, 2$. This allows us to write that

$$-\int_{\Omega_1} k_1 \Delta u_1 v_1 - \int_{\Omega_2} k_2 \Delta u_2 v_2 = \int_{\Omega_1} k_1 \nabla u_1 \cdot \nabla v_1 + \int_{\Omega_2} k_2 \nabla u_2 \cdot \nabla v_2$$
$$- k_1 \int_\gamma \frac{\partial u_1}{\partial n_1} v_1 - k_2 \int_\gamma \frac{\partial u_2}{\partial n_2} v_2$$

We observe that if $v_{1|\gamma} = v_{2|\gamma} = \eta$, then using the condition on the normal derivative we would find that

$$\int_{\Omega_1} k_1 \nabla u_1 \cdot \nabla v_1 + \int_{\Omega_2} k_2 \nabla u_2 \cdot \nabla v_2 = (f_1, v_1) + (f_2, v_2).$$

As such, we consider the continuous extension operator P_i from the interface to each domain Ω_i such that $(P_i\eta)_{|\gamma} = \eta$. In that case, given a function μ defined in γ[5], the identity above holds if we rewrite it in the form

$$\int_{\Omega_1} k_1 \nabla u_1 \cdot \nabla P_1 \mu + \int_{\Omega_2} k_2 \nabla u_2 \cdot \nabla P_2 \mu = (f_1, P_1\mu) + (f_2, P_2\mu).$$

Finally, for the continuity on the interface we just enforce that $u_1 = u_2$ on γ. The process above allow us to state the weak form of problem (3.13) in the result below.

Proposition 3.3.1. *Consider the set of equations* (3.13) *and the bilinear form* $a_i = (w_i, v_i) = (\nabla w_i, \nabla v_i)$. *Let*

$$V_i = \{v_i \in H^1(\Omega_i) : v_{i|\partial\Omega \cap \partial\Omega_i} = 0\};$$
$$V_i^0 = H_0^1(\Omega_i)$$
$$\Lambda = \{\eta \in H^{\frac{1}{2}}(\gamma) : \eta = v_{|\gamma} \text{ for some } v \in V^0\}$$

---

[5]A description of such function will be given below, when we formalize the weak form of the problem. For now assume that such extension has the regularity that we need.

where $V^0 = H_0^1(\Omega)$ as above. Then the weak formulation of (3.13) *reads as*

$$\textit{find } u_1 \in V_1, u_2 \in V_2 \textit{ such that } \begin{cases} a_1(u_1, v_1) = (\frac{f_1}{k_1}, v_1), \ \forall v_1 \in V_1^0 \\[2mm] a_2(u_2, v_2) = (\frac{f_2}{k_2}, v_1), \ \forall v_2 \in V_2^0 \\[2mm] u_1 = u_2, \ \textit{ on } \gamma \\[2mm] a_1(k_1 u_1, P_1\mu) + a_2(k_2 u_2, P_2\mu) = (f_1, P_1\mu) + (f_2, P_2\mu), \ \forall \mu \in \Lambda \end{cases}$$

<div align="right">(3.16)</div>

where the operator $P_i : \Lambda \to V_i$ is continuous for $i = 1, 2$.

Remark 3.3.2. *The existence of the (continuous) extension operators P_1 and P_2 is not obvious. See [40] or [5] for the existence of such operator.*

We are now ready to prove the equivalence between both problems:

Theorem 3.3.3. *Problem* (3.15) *is equivalent to* (3.16).

Proof. ($\Longrightarrow$) :

Let $u \in V^0$ be a solution of problem (3.15). We start by defining $u_1 = u_{\Omega_1}$ and $u_2 = u_{\Omega_2}$. It's clear that u_1 and u_2 satisfy equations 1 and 2 of (3.16).

For equation 3, we use the fact that $u \in H^1(\Omega)$ and therefore $u \in H^2_{\text{loc}}(\Omega)$. Given Ω' such that $\Omega' \Subset \Omega$ and $\gamma \subset \Omega'$, we have that $u \in H^2(\Omega')$ and $u \in C^{0,\lambda}(\overline{\Omega'})$ (u is in the Hölder Space of exponent λ; see Theorem 4.12 of [40] for more details.) As such, u is continuous on the interface and $u_1 = u_2$ on γ.

Finally, given $\mu \in \Lambda$, we can define the function

$$P\mu = \begin{cases} P_1\mu \\[2mm] P_2\mu \end{cases}$$

which satisfies $P\mu \in V^0$ and the equality 4 in (3.16).

($\Longleftarrow$) :

Let $u_1 \in V_1^0, u_2 \in V_2^0$ be the two solutions of problem (3.15). We now set

$$u = \begin{cases} u_1, \ \text{in } \Omega_1 \\[2mm] u_2, \ \text{in } \Omega_2 \end{cases} .$$

In this case, we again notice that for $i = 1, 2$ we have $u_i \in H^2_{\text{loc}}$ which implies that u_1 and u_2 is Hölder continuous and therefore u is also Hölder continuous since $u_1 = u_2$ on the interface, by assumption. Therefore, we also have that $u \in V^0$.

Defining $P\mu$ like above, we take $\mu \in \Lambda$ for some $v \in V$ such that $\mu = v_{|\gamma}$. As such, we have that the difference $(v_{|\Omega_i} - P_i\mu) \in V_i^0$ for each $i = 1, 2$ and

$$
\begin{aligned}
a(ku, v) &= \Big[a_1(k_1 u_1, v_{|\Omega_1} - P_1\mu) + a_1(k_1 u_1, P_1\mu)\Big] + \Big[a_2(k_2 u_2, v_{|\Omega_2} - P_2\mu) + a_2(k_2 u_2, P_2\mu)\Big] \\
&= \Big[(f_1, v_{|\Omega_1} - P_1\mu) + (f_1, P_1\mu)\Big] + \Big[(f_2, v_{|\Omega_2} - P_2\mu) + (f_2, P_2\mu)\Big] \\
&= (\tilde{f}, v), \implies a(u, v) = (f, v)
\end{aligned}
$$

where we take $\tilde{f} = \begin{cases} f_1, \text{ in } \Omega_1 \\ f_2, \text{ in } \Omega_2 \end{cases}$ as an auxiliary function and used the assumptions 1, 2 and 4 of equations (3.16). $\qquad\square$

Remark 3.3.4. *The above result is important because, as we will see, the Method of Fundamental Solutions only addresses the solution of each subdomain Ω_i independently (for which we have density and convergence results for functions in H^1) while enforcing the interface conditions. By the result above we're, in fact, in the conditions of our numerical method since each function belongs to a closed subspace of $H^1(\Omega_i)$ for $i = 1, 2$.*

<div style="text-align: right; font-size: 8em; color: #999;">4</div>

The Method of Fundamental Solutions

Contents

4.1 Density and linear independence results

The method of Fundamental Solutions is the base method to be implemented throughout this work. As a meshless method, it does not involve any kind of domain discretization (into some mesh) like in finite differences or finite elements methods. Instead, the problem is now of point placement. Since the mesh creation is one of the most computational expensive parts of the methods above, one of the main advantages of the MFS is exactly the lack of it.

As the name implies, MFS is based on the fundamental solutions of a previously known PDE. Consider the Elliptic linear differential operator $\mathcal{L}$ with fundamental solution Φ such that $\mathcal{L}\Phi(x) = \delta, \ \forall x \in \mathbb{R}^d$. Intuitively, we can consider the approximation

$$\tilde{u}(x) = \sum_{j=1}^{N} \alpha_j \Phi(x - y_j)$$

to the partial differential equation with a linear boundary operator $\mathcal{B}$

$$\begin{cases} \mathcal{L}u(x) = 0, x \in \Omega \\ \mathcal{B}u(x) = 0, x \in \partial\Omega \end{cases}.$$

By definition and using the linearity of the operator $\mathcal{L}$, $\tilde{u}$ satisfies the equation in Ω, and the coefficients α_j can be determined by imposing the boundary conditions

$$\mathcal{B}\tilde{u}(x) = \sum_{j=1}^{N} \alpha_j \mathcal{B}\Phi(x - y_j) = 0,$$

where $y_j \in \hat{\Gamma} \subset \mathbb{R}^d \setminus \overline{\Omega}$ with $j = 1, \ldots, N$, are the so-called source points to be chosen. We chose them to be outside our domain since, by translation, the Fundamental Solution Φ has a singularity at each y_j because, otherwise, it would render our approximation full of singularities inside Ω.

Remark 4.1.1. *While the motivation above might seem far-fetched, one can observe that the approximation $\tilde{u}$ resembles a convolution between some density function $\alpha(x)$ and the fundamental solution Φ. As we will see below, it can be proven that the fundamental solutions of the operator $\mathcal{L}$ are dense in the functional space defined in $\partial\Omega$ (which is enough since, as we already saw, the interior condition is satisfied by construction). For example, considering Dirichlet boundary conditions, one can use the single layer potential (which is going to be presented and studied in the next pages) that allow, through a discretization argument, to give a numerical approximation to the BVP and*

$$u(x) = \int_{\Gamma} \Phi(x - y)\varphi(y)d\sigma(y) \approx \sum_{j=1}^{N} w_j \varphi(y_j)\Phi(x - y_j) = \tilde{u}(x), \tag{4.1}$$

where $\varphi(y)$ is a layer density to be determined and $y_j \in \hat{\Gamma}$ and w_j are the nodes and weights of some quadrature, respectively. Setting $\mathcal{B} = I$ and $\alpha_j = w_j\varphi(y_j)$, we recover the approximation given above.

First, we introduce the notion of *artificial boundary* (or *pseudo-boundary*), which is analyzed in [41].

Definition 4.1.2. *A source set $\hat{\Gamma}$ is said to be admissible if*

1. *$\hat{\Gamma} \subset \mathbb{R}^d \setminus \overline{\Omega}$ is an open set with components in each external part of Ω;*

2. *$\hat{\Gamma} = \partial\hat{\Omega}$ is the boundary of $\hat{\Omega}$, where $\hat{\Omega} \subset \mathbb{R}^d \setminus \overline{\Omega}$ is an open set with components in each external part of Ω. Note that the problem must be well posed in $\hat{\Omega}$;*

3. *$\hat{\Gamma} \subset \partial\hat{\Omega}$, when $\partial\hat{\Omega}$ is an analytical boundary set verifying (2.) and $\hat{\Gamma}$ is open in the $\partial\hat{\Omega}$ topology.*

We denote the set of chosen source points by $\mathcal{Y} = \{y_j \in \hat{\Gamma} : j = 1, \ldots, N\}$.

Throughout this work, the adopted source set will always be the second option since it provides better numerical results. However, notice that the density results below still hold when considering different types of admissible source sets.

Assume that $\mathcal{L} = -\Delta$ and Φ is the fundamental solution of the Laplace equation. Until further notice, we are working with Dirichlet boundary conditions. Of course, the results stated below are also valid with different boundary conditions. In the appropriate functional space and given an admissible source set $\hat{\Gamma}$, consider the approximation space

$$\mathcal{S}(\Gamma, \hat{\Gamma}) = \mathrm{span}\{\Phi(x - y)_{|x \in \Gamma} : y \in \hat{\Gamma}\}.$$

Some preliminary results are going to be needed in order to present the desired density proofs. We start by introducing the concept of analytic continuation. For further details see [42].

Definition 4.1.3. *Let f be a complex valued function defined on $\Omega \subset \mathbb{C}$. We say that f is holomorphic on Ω if for every $a \in \Omega$, there exists a neighborhood U of a and $(c_n)_{n \in \mathbb{N}} \subset \mathbb{C}$ such that the power series*

$$\sum_{n=0}^{\infty} c_n(z - a)^n$$

converges to $f(z)$ for every $z \in U$.

Theorem 4.1.4 (Analytic continuation)**.** *Let f be a holomorphic function in the connected subset $\Omega \subset \mathbb{C}$. If there exists a non-empty $U \subset \Omega$ such that $f = 0$ in U, then $f = 0$ in Ω.*

As seen in the above remark, the study of layer potentials plays an important role in the Method of Fundamental Solutions, which are now formalized, and some results are stated. Since this is by itself a large topic see [13], [43] and [44] for more details.

Definition 4.1.5. *Let Ω be a bounded domain of class C^2 and $\varphi \in H^{\frac{1}{2}}(\Omega)$. The functions*

$$S\varphi(x) = \int_{\partial\Omega} \Phi(x-y)\varphi(y)d\sigma(y)$$

and

$$M\varphi(x) = \int_{\partial\Omega} \frac{\partial\Phi(x-y)}{\partial n}\varphi(y)d\sigma(y)$$

are called the single and double layer potentials with density φ, respectively.

Proposition 4.1.6. *Let Ω be a bounded domain of class C^2 and $\varphi \in H^{\frac{1}{2}}(\Omega)$. Then the single layer potential is harmonic in $\mathbb{R}^d \setminus \overline{\partial\Omega}$, continuous across $\partial\Omega$, and for every $x \in \partial\Omega$ we have the following jump relations for the normal derivative:*

$$\lim_{z \to x} \frac{\partial S\varphi}{\partial n^-}(z) = \int_{\partial\Omega} \frac{\partial\Phi(x-y)}{\partial n}\varphi(y)d\sigma(y) - \frac{1}{2}\varphi(x), \quad z \in \mathbb{R}^d \setminus \overline{\Omega}$$

and

$$\lim_{z \to x} \frac{\partial S\varphi}{\partial n^+}(z) = \int_{\partial\Omega} \frac{\partial\Phi(x-y)}{\partial n}\varphi(y)d\sigma(y) + \frac{1}{2}\varphi(x), \quad z \in \Omega.$$

In particular, we have

$$\varphi(x) = \frac{\partial S\varphi}{\partial n^+}(x) - \frac{\partial S\varphi}{\partial n^-}(x), \ \forall x \in \partial\Omega.$$

Analogously, the double layer potential is harmonic in $\mathbb{R}^d \setminus \overline{\partial\Omega}$, its normal derivative is continuous across $\partial\Omega$, and for every $x \in \partial\Omega$ we have the following jump relations:

$$\lim_{z \to x} M^+\varphi(z) = \int_{\partial\Omega} \frac{\partial\Phi(x-y)}{\partial n}\varphi(y)d\sigma(y) + \frac{1}{2}\varphi(x), \quad z \in \mathbb{R}^2 \setminus \overline{\Omega}$$

and

$$\lim_{z \to x} M^-\varphi(z) = \int_{\partial\Omega} \frac{\partial\Phi(x-y)}{\partial n}\varphi(y)d\sigma(y) - \frac{1}{2}\varphi(x), \quad z \in \Omega$$

In particular, we have

$$\varphi(x) = M^+\varphi(x) - M^-\varphi(x), \ \forall x \in \partial\Omega.$$

Lastly, it will be useful to study the well-posedness of the exterior Dirichlet problem for the Laplace Equation, c.f [45].

Theorem 4.1.7 (Well-Posedness of the Exterior Dirichlet problem)**.** *Let Ω be a bounded and open subset of $\mathbb{R}^2$. Then, there exists a unique solution $u \in C^2(\Omega^c) \cap C(\overline{\Omega^c})$ of the exterior Dirichlet Laplacian problem*

given by

$$\begin{cases} \Delta u = 0, \text{ in } \mathbb{R}^2 \setminus \overline{\Omega} \\ u = 0, \text{ on } \partial\Omega \\ u(x) = \mathcal{O}(1), \text{ for } |x| \to \infty. \end{cases}$$

Remark 4.1.8. *Notice that the condition at infinity must be enforced to have uniqueness. Otherwise, one could easily find a family of solutions up to a multiplicative constant (if $u(x)$ is a solution, then $\alpha u(x)$ would also be a solution for any $\alpha \in \mathbb{R}$).*

The main result which justifies the MFS for the Laplace equation is now stated. The proof given here is slightly different from the ones in [8], [41]. It is also influenced by the proofs in [46].

Theorem 4.1.9. *Let Ω be an open and bounded set with C^2 boundary $\Gamma = \partial\Omega$ such that $\overline{\Omega} \subset \hat{\Omega} \subset \mathbb{R}^2$, where $\hat{\Omega}$ is an open and bounded set and $\hat{\Gamma} = \partial\hat{\Omega}$ is an admissible source set. Then, $\mathcal{S}(\Gamma, \hat{\Gamma}) \oplus \mathbb{R}$ is dense in $H^{\frac{1}{2}}(\Gamma)$ and in $H^{-\frac{1}{2}}(\Gamma)$.*

Proof. In view of Lemma (2.1.10) we start by fixing some notation. Let $E = H^{\frac{1}{2}}(\Gamma)$. For every (fixed) $y \in \hat{\Gamma}$, the maps

$$\Phi(\cdot - y) : \varphi \mapsto \int_\Gamma \Phi(x - y)\varphi(x)d\sigma(x)$$

$$1 : \varphi \mapsto \int_\Gamma \varphi(x)d\sigma(x)$$

are linear and continuous in $H^{\frac{1}{2}}(\Gamma)$, and $1, \Phi(\cdot - y) \in H^{-\frac{1}{2}}(\Gamma)$ (notice that $1, \Phi(\cdot - y) \in L^1_{\text{loc}}(\mathbb{R}^2)$ and $1, \Phi(\cdot - y) \in L^2(\hat{\Gamma})$).

Observe that $\mathcal{S}(\Gamma, \hat{\Gamma}) \oplus \mathbb{R} = \text{span}\{1, \Phi\}$ and let $N = \text{span}\{1, \Phi\} \subset H^{-\frac{1}{2}}(\Gamma)$. Using the Definition (2.1.9),

$$N^\perp = \{\varphi \in H^{\frac{1}{2}}(\Gamma) : \langle\psi, \varphi\rangle = 0, \ \forall\psi \in N\}$$

our goal is to prove that $N^\perp = \{0\}$. Let $\varphi \in N^\perp$ and consider $w(y) = \int_\Gamma \Phi(x - y)\varphi(x)d\sigma(x), \ y \in \mathbb{R}^2$. Then,

$$\int_\Gamma \Phi(x - y)\varphi(x)d\sigma(x) = 0, \ \forall y \in \hat{\Gamma} \tag{4.2}$$

and

$$\int_\Gamma \varphi(x)d\sigma(x) = 0. \tag{4.3}$$

In order to verify that $w(y)$ satisfies the exterior Laplace problem with Dirichlet boundary conditions, one can use the fact that w exhibits the asymptotic behavior

$$w(y) = -\frac{1}{2\pi} \int_\Gamma \varphi(x)d\sigma(x) \log|y| + \mathcal{O}(1), \ |y| \to \infty$$

43

and condition (4.3), to check that w is bounded at infinity. Therefore, by condition (4.2)

$$\begin{cases} \Delta w = 0, \text{ in } \mathbb{R}^2 \setminus \hat{\Omega} \\ w(y) = 0, \text{ on } \hat{\Gamma} \\ w(y) = \mathcal{O}(1), |y| \to \infty. \end{cases}$$

Since the problem above is well-posed, its unique solution is $w(y) = 0, \ \forall y \in \mathbb{R}^2 \setminus \overline{\hat{\Omega}}$. By (a unique) analytic continuation (see Theorem (4.1.4)), we can extend w by zero in $\mathbb{R}^2 \setminus \overline{\Omega}$. Since w is a single layer potential over Γ, w is continuous on Γ and therefore, by continuity, $w = 0$ on Γ. Once again, using the fact that the single layer potential is harmonic in Ω, w satisfies the (inner) Laplace problem

$$\begin{cases} \Delta w = 0, \text{ in } \Omega \\ w(y) = 0, \text{ on } \Gamma \end{cases}$$

which, by uniqueness, implies that $w = 0$ in $\hat{\Omega}$. Finally, we can conclude that $\varphi = 0$ in Γ by Proposition (4.1.6) since the normal derivate jump is zero.

Therefore, we can write $N^{\perp} = \{0\}$ and by Lemma (2.1.10)

$$\mathcal{S}(\Gamma, \hat{\Gamma}) \oplus \mathbb{R} = \overline{\text{span}\{1, \Phi\}} = \{0\}^{\perp}$$

given the fact that $H^{\frac{1}{2}}(\Omega)$ is reflexive. Since $0 \in H^{\frac{1}{2}}(\Gamma)$ (and $0 \in H^{-\frac{1}{2}}(\Gamma)$) then $\mathcal{S}(\Gamma, \hat{\Gamma}) \oplus \mathbb{R}$ is dense in $H^{\frac{1}{2}}(\Gamma)$ and in $H^{-\frac{1}{2}}(\Gamma)$ (this is to be expected since $H^s(\Omega)$ is dense in $H^{-s}(\Omega)$ for $s > 0$). $\qquad \square$

Remark 4.1.10. *The proof above guarantees the existence of a sequence of density layers $\{\varphi_n\} \subset H^{\frac{1}{2}}(\Gamma)$ and a sequence of constants $\{c_n\} \subset \mathbb{R}$ such that the modified single layer potential*

$$\hat{\mathcal{S}}\varphi_n(y) = \int_{\hat{\Gamma}} \Phi(x - y)\varphi_n(x)d\sigma(x) + c_n$$

converges to the Dirichlet boundary data $g(y)$ in $H^{\frac{1}{2}}(\Gamma)$, i.e,

$$\left\| \hat{\mathcal{S}}\varphi_{n|\Gamma} - g \right\|_{H^{\frac{1}{2}}(\Gamma)} \to 0, \ n \to \infty.$$

Since $\hat{\mathcal{S}}\varphi_n$ is harmonic for each $n \in \mathbb{N}$, every interior Dirichlet BVP can be approximated using the modified single layer potential. Conversely, any $\varphi \in H^{\frac{1}{2}}(\Gamma)$ and $c \in \mathbb{R}$ define a BVP whose solution is given by the associated modified single layer potential $\hat{\mathcal{S}}\varphi(y)$, with boundary data given by its restriction to Γ.

Finally, the discretization argument to be presented follows from the fact that, given a set of source

points $\mathcal{Y} = \{y_1, \ldots, y_N\} \subset \mathbb{R}^2 \setminus \overline{\Omega}$, the fundamental solutions $\Phi(\cdot - y_1), \ldots, \Phi(\cdot - y_N)$ are linearly independent on $\partial\Omega$ and therefore in Ω.

Theorem 4.1.11. *Let $\mathcal{Y}$ be a set of source points, as defined above. Then, the restriction of the functions $\Phi(\cdot - y_1), \ldots, \Phi(\cdot - y_N)$ to $\partial\Omega$ are linearly independent.*

Proof. Assume that $\tilde{u}(x) = \sum_{j=1}^{N} \alpha_j \Phi(x - y_j) = 0, \ \forall x \in \partial\Omega$. We prove that $\alpha_1 = \cdots = \alpha_N = 0$. Since, by construction, $\tilde{u}$ satisfies the Laplace equation and by assumption $\tilde{u}(x) = 0, \ \forall x \in \partial\Omega$, by the well-posedness of the interior Dirichlet problem, $\tilde{u} = 0$ in $\overline{\Omega}$. Again, by analytic continuation, $\tilde{u} = 0$ in $\mathbb{R}^2 \setminus \mathcal{Y}$. Applying the Laplace operator to $\tilde{u}$, by linearity

$$\sum_{j=1}^{N} \alpha_j \delta y_j = 0$$

which implies that $\alpha_1 = \cdots = \alpha_N = 0$ by the linear independence of the Dirac deltas. $\qquad\square$

Consider now the operator $\mathcal{L} = -(\Delta + k^2)$, and assume that k is **not** an eigenfrequency of the Helmholtz equation. The results presented for the fundamental solution of the Laplace Equation still hold for the fundamental solution of the Helmholtz equation. However, a different type of infinity conditions must be considered, the so-called *Sommerfeld Radiation Conditions*, c.f [44].

Theorem 4.1.12 (Well-Posedness of the Exterior Dirichlet problem of the Helmholtz Equation)**.** *Let Ω be a bounded and open subset of $\mathbb{R}^2$. Then, there exists a unique solution $u \in C^2(\Omega^c) \cap C(\overline{\Omega^c})$ of the exterior Dirichlet Helmholtz problem given by*

$$\begin{cases} -\Delta u = k^2 u, \ \text{in } \mathbb{R}^2 \setminus \overline{\Omega} \\ u = 0, \ \text{on } \partial\Omega \\ |x| \left(\frac{x}{|x|} \nabla u(x) - ik \right) u(x) = 0, \ \text{for } |x| \to \infty. \end{cases}$$

Remark 4.1.13. *Just like the exterior Dirichlet problem for the Laplace Equation, the Well-Posedness of the exterior Helmholtz Problem depends on the conditions at infinity. In this case, they are known as Sommerfeld Radiation Conditions and are of the form*

$$|x|^{\frac{d-1}{2}} \left(\frac{x}{|x|} \nabla u(x) - ik \right) u(x) = 0, \ \text{for } |x| \to \infty,$$

where d stands for the space dimension. We also notice that the single layer potential given by

$$\int_{\Gamma} \Phi_k(x - y)\varphi(x) d\sigma(x)$$

satisfies the Sommerfeld Radiation Condition, when $|y| \to \infty$.

45

Analogously to the Laplace problem, consider the space

$$\mathcal{S}(\Gamma, \hat{\Gamma}) = \operatorname{span}\{\Phi_k(x - y)_{|x \in \Gamma} : y \in \hat{\Gamma}\}.$$

Again, like in Theorem (4.1.9), we point the reader to [41], [46] and [47], where slightly different proofs are stated.

Theorem 4.1.14. *Let Ω be an open and bounded set with C^2 boundary $\Gamma = \partial\Omega$ such that $\overline{\Omega} \subset \hat{\Omega} \subset \mathbb{R}^2$, where $\hat{\Omega}$ is an open and bounded set and $\hat{\Gamma} = \partial\hat{\Omega}$ is an admissible source set. Then, $\mathcal{S}(\Gamma, \hat{\Gamma})$ is dense in $H^{\frac{1}{2}}(\Gamma)$ and in $H^{-\frac{1}{2}}(\Gamma)$.*

Proof. This proof follows the same steps as in the proof of Theorem (4.1.9). Let $E = H^{\frac{1}{2}}(\Gamma)$. For every (fixed) $y \in \hat{\Gamma}$, the map

$$\Phi_k(\cdot - y) : \varphi \mapsto \int_\Gamma \Phi_k(x - y)\varphi(x)d\sigma(x)$$

is linear and continuous in $H^{\frac{1}{2}}(\Gamma)$ and $\Phi_k(\cdot - y) \in H^{-\frac{1}{2}}(\Gamma)$. Let $N = \operatorname{span}\{\Phi_k(\cdot - y)\}$ and

$$N^\perp = \{\varphi \in H^{\frac{1}{2}}(\Gamma) : \langle \psi, \varphi \rangle = 0, \psi \in N\}.$$

Once again, we prove that $N^\perp = \{0\}$, i.e, it suffices to prove that given $\varphi \in H^{\frac{1}{2}}(\Gamma)$ the implication

$$\forall y \in \hat{\Gamma}, \int_\Omega \Phi_k(x - y)\varphi(x)d\sigma(x) = 0 \implies \varphi(x) = 0, \ \forall x \in \mathbb{R}^2$$

holds. Define

$$w(y) = \int_\Gamma \Phi_k(x - y)\varphi(x)d\sigma(x).$$

Given that w satisfies the Sommerfeld Radiation Conditions and, by assumption, $w(y) = 0$ in $\hat{\Gamma}$, then $w = 0$ in Ω is the unique solution of the exterior Dirichlet problem of the Helmholtz equation

$$\begin{cases} -\Delta w = k^2 w, \text{ in } \mathbb{R}^2 \setminus \overline{\Omega} \\ w = 0, \text{ on } \partial\Omega \\ |y|(\frac{y}{|x|}\nabla w(y) - ik)u(x) = 0, \text{ for } |y| \to \infty, \end{cases}$$

since k is not an eigenfrequency. By analytic continuation, we can extend w by zero to $\mathbb{R}^2 \setminus \overline{\Omega}$. The rest of the proof is the same as in the Theorem (4.1.9), using the fact that k is not an eigenfrequency and the interior Dirichlet problem is well posed. $\qquad\square$

Remark 4.1.15. *Both in Theorem (4.1.9) and Theorem (4.1) the density proof can generalize to $H^s(\Gamma)$, for $s \geq \frac{1}{2}$. However, in applications, we are only interested in the case $s = \frac{1}{2}$. Notice that if $s = 0$, it is*

not required to invoke the Hahn-Banach Theorem since $H^0(\Gamma) = L^2(\Gamma)$ which is a Hilbert Space, and it would suffice to use Corollary (2.2.3). For general boundary conditions, the proofs above follow the same argument, where one should consider the appropriate approximating set $\mathcal{S}(\Gamma, \hat{\Gamma})$ and the appropriate integral operator (for example, for Neumann boundary conditions, one should consider the set

$$\mathcal{S}(\Gamma, \hat{\Gamma}) = \mathrm{span}\{\partial_n \Phi(x - y)_{|x \in \Gamma} : y \in \hat{\Gamma}\}$$

and the double layer potential $M\varphi$, and recall that $\partial_n u = g \in H^{-\frac{1}{2}}(\Gamma)$).

Once again, the discretization argument follows from the linear independence of the functions $\Phi_k(\cdot - y_1), \ldots, \Phi_k(\cdot - y_1)$, where $y_1, \ldots, y_N \in \mathbb{R}^2 \setminus \overline{\Omega}$ are distinct source points. The proof is identical to the one presented in Theorem (4.1.11), where we use the fact that k is not an eigenfrequency.

Before stating some results regarding the convergence and the stability of the MFS for the Laplace and Helmholtz equations, we address the problem of the source points placement. Although different methods can be considered, e.g. [41], throughout this work we place the artificial boundary $\hat{\Gamma}$ over the boundary of Ω. To be more precise, consider $\Gamma = \partial\Omega$ and the (equally spaced) colocation points $x_1, \ldots, x_M \in \Gamma$. Then, we approximate the (outward) normal vector $\tilde{n}_i$ to the point x_i, which is given by

$$\tilde{\mathbf{n}}_i = \frac{(x_i - x_{i-1})^\perp}{2} + \frac{(xx_{i+1} - x_i)^\perp}{2},$$

with the orthogonal notation $z^\perp = (-z_2, z_1)$. This way, one can approximate the unit normal vector by $\mathbf{n} = \frac{\tilde{\mathbf{n}}}{|\tilde{\mathbf{n}}|}$ and define the source point y_i by

$$y_i = x_i + \eta\mathbf{n},$$

where $\eta > 0$ is some small coefficient which controls the distance from each point in Γ and $\hat{\Gamma}$. As we shall see below, this coefficient has an important impact on the convergence of the MFS, where bigger values of η produce better approximations. However, this is only feasible for simple geometries, because it also increases the condition number of matrix A, denoted by $\kappa(A)$.

4.2   Numerical approach for the Laplace Equation

Given the results above, it is possible to numerically solve the Laplace and Helmholtz equations for any boundary data $g(x)$ if we are able to find the coefficients in the discretization of the single layer potential. For simplicity, we still assume Dirichlet boundary conditions. Let N be the number of source points and M the number of colocation points on the boundary, denoted by $x_1, \ldots, x_i, \ldots, x_M$ with $i = 1, \ldots, M$.

Then, we solve the discretized equation

$$\tilde{u}(x_i) = \sum_{j=1}^{N} \alpha_j \Phi(x - y_j) + \alpha_{N+1} = g(x_i)$$

with respect to the coefficients α_j. Defining $g_i := g(x_i)$, $i = 1, \ldots, M$, notice that the equation above can be rewritten in the matricial form

$$\underbrace{\begin{bmatrix} \Phi(x_1, y_1) & \cdots & \Phi(x_1, y_N) & 1 \\ \vdots & \ddots & \vdots & \vdots \\ \Phi(x_M, y_1) & \cdots & \Phi(x_M, y_N) & 1 \end{bmatrix}}_{A \quad M \times (N+1)} \underbrace{\begin{bmatrix} \alpha_1 \\ \vdots \\ \alpha_N \\ \alpha_{N+1} \end{bmatrix}}_{\alpha \quad (N+1) \times 1} = \underbrace{\begin{bmatrix} g_1 \\ \vdots \\ g_M \end{bmatrix}}_{g \quad M \times 1} \tag{4.4}$$

This problem can be framed in two different ways:

- if $N + 1 = M$, then we are faced with an interpolation problem, where we solve a linear system of N equations and N unknowns;

- if $M > N + 1$, then we must solve a least-squares problem. Observe that the case $M < N + 1$ is an under determined system of equations and therefore the number of colocation points must be greater that the number of source points. In any case, every numerical linear algebra software is able to solve this type of problem efficiently. This is the method used in this work, since it avoids interpolation instabilities, forces the boundary condition to hold at some specific points and is particularly robust when dealing with non-regular boundary data. After several numerical experiments, e.g. [41], it was concluded that $N = 2M$ is a good choice for the number of source points.

Notice that different boundary conditions can be considered: for example, if solving the Laplace equation with Neumann boundary conditions, one should replace the entries $\Phi(x_i, y_j)$ with $\partial_{n_x} \Phi(x_i, y_j) = \nabla_x \Phi(x_i, y_j) \cdot n$, where n is the unit normal vector to the boundary in the point x_i.

We now state some results regarding the convergence and the stability of the MFS for the Laplace equation with Dirichlet boundary conditions. Here, we state this results when the domain Ω is a disk and the artificial boundary $\hat{\Gamma} = \partial\hat{\Omega}$ that involves Ω is also a circle. Let ρ be the radius of Ω, R the radius of $\hat{\Omega}$ and assume that $N = M$.

Theorem 4.2.1. *Assume that $R^N - \rho^N \neq 1$. Then,*

1. *the matrix A is non-singular;*

2. *if $R \neq 1$ and the boundary data g is real and analytic we can also prove that the exact solution u of the Laplace equation admits a harmonic extension to some neighborhood of $\overline{\Omega}$. Therefore, we*

may assume that u is harmonic in $0 \leq r \leq r_0$ for some $r_0 \geq \rho$. In this case, there exists $C > 0$ and $c \in (0, 1)$ which are independent of N and u such that

$$\sup_{x \in \overline{\Omega}} |u(x) - \tilde{u}(x)| \leq C c^N \sup_{|x| \leq r_0} |u(x)|.$$

The Theorem above provides some important insights regarding the MFS. First, we cannot fail to notice that this method displays *exponential convergence* in the number of source points, which is quite remarkable. In fact, the term c depends on the distance between Γ and the artificial boundary $\hat{\Gamma}$, which is controlled by the coefficient η, and

$$c = \begin{cases} \frac{\rho}{R}, & \text{if } r_0 > \frac{R^2}{\rho} \\ \sqrt{\frac{\rho}{R}}, & \text{if } r_0 < \frac{R^2}{\rho}. \end{cases}$$

Unfortunately, one of the main drawbacks of the MFS is the ill-condition of the matrix A and the fact that the matrix A is very dense, and we cannot use optimized sparse software solvers on the system (4.4). In particular, while bigger values of the parameter η allows for better numerical approximations it also implies an exponential growth of the condition number $\kappa(A)$, see [48], [49] and [50].

Theorem 4.2.2. *In the conditions of the Theorem (4.2.1), the condition number can be estimated by*

$$\kappa(A) \sim \frac{\log R}{2} N \left(\frac{R}{\rho} \right)^{\frac{N}{2}}.$$

Another interesting remark, is the condition $R \neq 1$, which is in direct connection with the space $\mathcal{S}(\Gamma, \hat{\Gamma}) \oplus \mathbb{R}$ that was proven to be dense in $H^{\frac{1}{2}}(\Gamma)$ in Theorem (4.1.9). Assume that $R = 1$ and $\hat{\Omega}$ is a disk with radius R that contains the origin. Then, if one does not consider the constant basis function 1,

$$\tilde{u}(0) = \sum_{j=1}^{N} \alpha_j \Phi(0 - y_j) = -\frac{1}{2\pi} \sum_{j=1}^{N} \alpha_j \log(R) = 0,$$

no matter the choice of the source points over $\hat{\Gamma}$. Therefore, it is impossible to approximate any harmonic function which does not vanish on the origin. However, this is not the case if we add the basis function 1, which was used to prove the density result. While this almost never interferes with the numerical approximations in the next chapters, it will be considered nevertheless by a reason of coherence. This is the reason why a column of ones was added in the matrix A.

4.2.1 An enrichment technique

Before diving into the numerical approach for the Helmholtz equation, we introduce some modifications to the classical MFS method presented above. There is another drawback in our method: our basis

functions are analytical and might lose precision when approximating functions which display singularities, for example near a corner if the domain is not smooth. In what follows we introduce an enrichment technique which allows for singularity treatment. In the same vein as in the Proposition (3.2.3), we reintroduce the notion of a wedge domain and consider some wedge like domain with interior angle Θ.
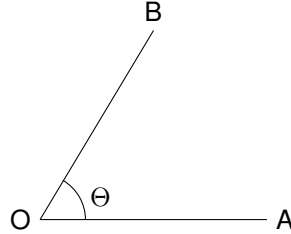

Figure 4.1: A wedge domain with an interior angle Θ.

Consider the Laplace equation in polar coordinates, given by

$$\left(\partial_r^2 + \frac{1}{r}\partial_r + \frac{1}{r^2}\partial_\theta^2\right) u(r,\theta) = 0, \quad r > 0,\ 0 \leq \theta \leq \Theta. \tag{4.5}$$

Then, by separation of variables $u(r,\theta) = R(r)T(\theta)$, one can find two different families of particular solutions given by,

$$u(r,\theta) = \left(c_1 r^\alpha + c_2 r^{-\alpha}\right) \times \left(c_3 \cos(\alpha\theta) + c_4 \sin(\alpha\theta)\right), \ \alpha > 0$$

and

$$u(r,\theta) = \left(c_1 \log(r) + c_2\right) \times \left(c_3 \cos(\alpha\theta) + c_4 \sin(\alpha\theta)\right), \ \alpha = 0$$

where $c_1, c_2, c_3, c_4 \in \mathbb{C}$. In order to find α, one must consider the amplitude of the angle Θ and the boundary conditions at each segment $\overrightarrow{OA}$ and $\overrightarrow{OB}$. Below we summarize the asymptotic harmonic solutions of (4.5). For more details we point the reader to [1].

- For Dirichlet-Dirichlet boundary conditions given by $u(r,0) = A, u(r,\Theta) = B$, then $\alpha_k = \frac{k\pi}{\Theta}$ and

$$u(r,\theta) = A(B-A)\frac{\theta}{\Theta} + \sum_{k=0}^{\infty} \alpha_k r^{\alpha_k} \sin(\alpha_k\theta);$$

- For Dirichlet-Neumann boundary conditions given by $u(r,0) = A, \partial_n u(r,\Theta) = B$, then $\alpha_k = \frac{\left(k+\frac{1}{2}\right)\pi}{\Theta}$ and

  - If $\Theta \neq \frac{\pi}{2}, \frac{3\pi}{2}$,

$$u(r,\theta) = A + \frac{B}{\cos(\Theta)} r \sin(\theta) + \sum_{k=0}^{\infty} \alpha_k r^{\alpha_k} \sin(\alpha_k\theta);$$

– If $\Theta = \frac{\pi}{2}, \frac{3\pi}{2}$,

$$u(r,\theta) = A + (-1)^{l+1}\frac{Br}{\Theta}\left(\log(r)\sin(\theta) + \theta\cos(\theta)\right) + \sum_{k=0}^{\infty}\alpha_k r^{\alpha_k}\sin(\alpha_k\theta),$$

with $l = 0$ if $\Theta = \frac{\pi}{2}$ and $l = 1$ if $\Theta = \frac{3\pi}{2}$;

- For Neumann-Dirichlet boundary conditions given by $\partial_n u(r,0) = A, u(r,\Theta) = B$, then $\alpha_k = \frac{\left(k+\frac{1}{2}\right)\pi}{\Theta}$ and

– If $\Theta \neq \frac{\pi}{2}, \frac{3\pi}{2}$,

$$u(r,\theta) = B - Ar\sin(\theta) + \frac{A\sin(\Theta)}{\cos(\Theta)}r\cos(\theta) + \sum_{k=0}^{\infty}\alpha_k r^{\alpha_k}\cos(\alpha_k\theta);$$

– If $\Theta = \frac{\pi}{2}, \frac{3\pi}{2}$,

$$u(r,\theta) = B - \frac{Ar}{\Theta}\left(\log(r)\cos(\theta) - \theta\sin(\theta)\right) - Ar\sin(\theta) + \sum_{k=0}^{\infty}\alpha_k r^{\alpha_k}\cos(\alpha_k\theta);$$

- For Neumann-Neumann boundary conditions given by $\partial_n u(r,0) = A, \partial_n u(r,\Theta) = B$, then $\alpha_k = \frac{k\pi}{\Theta}$ and

– If $\Theta \neq \pi, 2\pi$,

$$u(r,\theta) = -Ar\sin(\theta) - \frac{B + A\cos(\Theta)}{\sin(\Theta)}r\cos(\theta) + \sum_{k=0}^{\infty}\alpha_k r^{\alpha_k}\cos(\alpha_k\theta);$$

– If $\Theta = \pi, 2\pi$,

$$u(r,\theta) = -Ar\sin(\theta) + \frac{(-1)^l B - A}{\Theta}r\left(\log(r)\cos(\theta) - \theta\sin(\theta)\right) + \sum_{k=0}^{\infty}\alpha_k r^{\alpha_k}\cos(\alpha_k\theta);$$

with $l = 0$ if $\Theta = \pi$ and $l = 1$ if $\Theta = 2\pi$.

Remark 4.2.3. *Observe that if the wedge domain is rotated by some angle θ_1 (see Figure (4.2)) one can consider the translation $\theta^\star = \theta - \theta_1$, where $\theta^\star$ is the angle on the "correct" wedge domain, see Figure (4.1).*
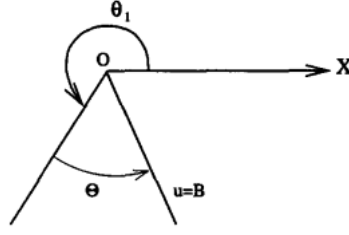
Figure 4.2: Rotation of the wedge domain. Image taken from [1].

In applications, we are mostly concerned with Dirichlet-Dirichlet, Dirichlet-Neumann and Neumann-Dirichlet boundary conditions. Just like stated above, some of these boundary conditions have different expansions for the angles $\Theta = \frac{\pi}{2}$ and $\Theta = \frac{3\pi}{2}$. However, we are only concerned with the expansion

$$v(r,\theta) = \sum_{k=0}^{\infty} \alpha_k r^{\alpha_k} \psi(\alpha_k \theta)$$

where $\psi = \sin$ or $\psi = \cos$. In these cases, if we neglect the other terms, for the special angle $\Theta = \frac{\pi}{2}$ above we would find that $\alpha_k \in \mathbb{N}$. Without going in dept in singularity analysis, then its partial derivative $\partial_r v(r, \theta)$ would be of the form

$$\partial_r v(r,\theta) = \sum_{k=0}^{\infty} \alpha_k^2 r^{\alpha_k - 1} \psi(\alpha_k \theta)$$

where $\alpha_k - 1 \in \mathbb{N}$. In general, if $\alpha_k \in \mathbb{N}$ for some angle Θ then all of its derivatives are continuous and $v(r,\theta)$ is analytical. More precisely, there is no singularity in these cases. Therefore, one does not need to enrich the set of basis functions since the fundamental solutions correctly reproduce the behavior near the corner's tip. Such corners are called regular. On the other hand, corners which present singularities are called singular and are the ones which we are interested to better approximate.

Also notice that, in the expansions above, the term $r^{-\alpha_k}$ does not appear. This has to do with the fact we are dealing with an interior problem: when considering the exterior problem, the terms r^{α_k} are replaced with $r^{-\alpha_k}$ (observe that it satisfies the asymptotic conditions prescribed in order to have well-posedness!).

To incorporate the singular behavior near a singular corner, first assume, without loss of generality, that the domain Ω has just one corner and that the solution of our BVP can be decomposed in regular and singular parts,

$$u(x) = u_R(x) + u_S(x), \ x \in \overline{\Omega},$$

where u_R is the regular part is approximated by the MFS basis functions, and the singular part u_S is approximated by the expansions above, having the boundary conditions into account. Let $\phi_s(r, \theta)$ be one of those expansions centered at the corner's tip, where s is the order of the expansion. Then, the

numerical approximation can be written as

$$\tilde{u}(x) = \sum_{j=1}^{N} \alpha_j \Phi(x - y_j) + \alpha_{N+1} + \sum_{s=1}^{p} \beta_s \phi_s(r(x), \theta(x)), \ x \in \overline{\Omega}. \tag{4.6}$$

Considering the collocation points $x_1, \ldots, x_M \in \partial\Omega$, the linear system of equations (4.4) can be generalized to

$$\underbrace{\left[\ A_1 \ | \ B_1 \ \right]}_{A} {}_{M \times (N+1+P)} \begin{bmatrix} \alpha \\ \beta \end{bmatrix}_{(N+1+P) \times 1} = \begin{bmatrix} \ g \ \end{bmatrix}_{M \times 1}, \tag{4.7}$$

where the block matrix A_1 is the matrix A in (4.4) and the B_1 block matrix is given by

$$B_1 = \begin{bmatrix} \phi_1(r(x_1), \theta(x_1)) & \cdots & \phi_p(r(x_1), \theta(x_1)) \\ \vdots & \ddots & \vdots \\ \phi_1(r(x_M), \theta(x_M)) & \cdots & \phi_p(r(x_M), \theta(x_M)). \end{bmatrix}$$

4.3   Numerical approach for the Helmholtz Equation

For the Helmholtz equation, the MFS convergence and stability results resemble the previous ones for the Laplace equation with Dirichlet boundary conditions. Once again, the results are stated for identical geometries as before, where Ω is the unit disk and the radius of $\hat{\Omega}$ is $R > 1$. Here is assumed that the boundary data g can be analytically extended to the annulus $\{z \in \mathbb{C} : \frac{1}{\rho} < |z| < \rho\}$, where $\rho > 1$. The following result is due to [51].

Theorem 4.3.1. *Let $R > 1$ and N be an even number. Then the minimum boundary error achieved by the MFS in the unit disk satisfies*

$$\left\| g - \tilde{u}_{|\Gamma} \right\|_{L^2(\Gamma)} \leq \begin{cases} C\rho^{-\frac{N}{2}}, \ \text{if } \rho < R^2 \\ C\sqrt{N}R^{-N}, \ \text{if } \rho = R^2 \\ CR^{-N}, \ \text{if } \rho > R^2 \end{cases}$$

where C is a constant that not depends on N.

To solve the Helmholtz equation with the MFS, one must start by computing the eigenvalues λ (or the eigenfrequencies k, with $\lambda = k^2$) first. In order to achieve that, recall that the Helmholtz equation

$$\begin{cases} -\Delta u = k^2 u, \ \text{in } \Omega \\ u = 0, \ \text{on } \partial\Omega \end{cases} \tag{4.8}$$

is well-posed when λ is not an eigenvalue, and in that case the nullspace of the single layer potential

operator

$$S_k\varphi(y) = \int_{\hat{\Gamma}} \Phi_k(x - y)\varphi(x)d\sigma(x)$$

is trivial. More precisely, one can prove the following result, e.g. [52].

Theorem 4.3.2. *If k is not an eigenfrequency of the interior Dirichlet problem, then $\dim(N(S_k)) = 0$.*

Proof. If k is not an eigenfrequency, then the interior problem is well posed which implies that $\varphi(x) = 0$, $x \in \overline{\Omega}$. By analytical continuation, $\varphi(x) = 0$, $x \in \hat{\Omega}$. Since the single layer potential is continuous, then $\varphi(x) = 0$, $x \in \hat{\Gamma}$. By the well-posedness of the exterior problem (notice that the single layer potential satisfies the Sommerfeld radiation conditions), then $\varphi(x) = 0$, $\forall x \in \mathbb{R}^2$. □

This theorem can be used to search for the eigenvalues/eigenfrequencies of the Laplace operator. By virtue of the discretization of the single layer potential (4.1), one should find the values k such that the nullspace of the matrix $A(k) = \left[\Phi_k(x_i - y_j)\right]_{M \times N}$ is not trivial. Like it was discussed in the previous section 4.2, that can be done in two different ways:

1. if $A(k)$ is a square matrix (with $M = N$), one can compute the determinant of $A(k)$. Since the components of $A(k)$ are complex numbers, then its determinant is also a complex number, and we consider its absolute value. In any case, instead of working with $|\det A(k)|$, since this value is very small, one must work with its logarithm and consider the function $d(k) = \log|\det A(k)|$;

2. if $A(k)$ is an $M \times N$ rectangular matrix, with $M > N$, one considers the smallest singular value, which we denote by $\sigma_N(k)$, where the singular values of $A(k)$ are assumed to be in decreasing order $\sigma_1(k) \geq \cdots \geq \sigma_N(k)$. We emphasize that we only work with this case.

Therefore, in order to find the eigenvalues/eigenfrequencies of the Laplace operator, one must find the singularities of the functions $d(k)$ or $\sigma_N(k)$ for the first and second cases above, respectively, i.e, study the local minima of the functions $d(k)$ or $\sigma_N(k)$ which, in very regular domains, should approach zero.

To search for these singularities, a simple direct search algorithm was developed to bracket the set of local minima in a given interval. The iterative algorithm used is based on the Golden Ratio Search already used in [52]. First, consider the graph of $\sigma_N(k)$ in a given interval $I = (a, b)$ (which likely has more than one local minima) and fix (a relatively large) step size h. Let $I_{M_0}^0 = \{a_0^0, \ldots, a_{M_0}^0\}$ be the discretization of $I_{M_0}^0$ in M_0 points spaced by h in the zeroth iteration, and denote the set of local minimums of I_{M_0} by $X_K^0 = \{x_0^0, \ldots, x_K^0\} \subset I_{M_0}$, i.e, $\forall i = 1, \ldots, K$ there exists $c^0, d^0 \in I_{M_0}^0$ such that $c^0 = x_i^0 - h$, $d^0 = x_i^0 + h$ and $x_i < \min(c^0, d^0)$. Then, for each x_i^0, $I_{M_0}^0$ is enlarged with the middle points between c^0 and x_i^0, d^0 and x_i^0, and it is denoted by $\tilde{I}_{M_1}^1$ (notice that $M_0 < M_1$)[1]. Finally, we sort $\tilde{I}_{M_1}^1$ in an increasing order and repeat the process for a specified depth d. When the maximum depth is

---

[1] Given the nature of the algorithm, one can also consider the left adjacent point to c^0, which we denote by $e_0 \in I_{M_0}^0$, compute and add their middle point to $\tilde{I}_{M_1}^1$

attained, one was able to successfully find small intervals which bracket *each local minimum* of σ_N in I, and it is now possible to apply a direct search method to find it to any desired precision: in this work, Brent's method was used [53], although Golden Ratio Search is also possible. The general form of the algorithm is given below.

Algorithm 4.1: Direct Bracketing Algorithm

Set maximum depth d
Set step size h
Set bracketing interval $I = (a, b)$
begin
    Discretize I into $I_{M_0}^0 = \{a_0^0, \ldots, a_{M_0}^0\}$, where $a_{j+1} = a_j + h$ for each $j = 1, \ldots M_0$
    Set $s = 0$

    (Bracketing step)
    while $s < d$ **do**
        Compute $X_{K_s}^s = \{x_0^s, \ldots, x_{K_s}^s\}$, the set of local minima of $I_{M_s}^s$
        Let E be an empty array
        foreach $x \in X_{K_s}^s$ **do**
            Consider the adjacent points to x given by $c, d \in I_{M_s}^s$ such that $c < x < d$
            Consider the left adjacent point to c, denoted by e
            Compute $\tilde{c} = \frac{c+x}{2}$
            Compute $\tilde{d} = \frac{d+x}{2}$
            Compute $\tilde{e} = \frac{e+c}{2}$
            Append $\tilde{c}, \tilde{d}$ and $\tilde{e}$ to E
        Let $\tilde{I}_{M_{s+1}}^{s+1} = I_{M_s}^s \cup E$
        Define $I_{M_{s+1}}^{s+1} = sort(\tilde{I}_{M_{s+1}}^{s+1})$
        $s \leftarrow s + 1$

    (Direct search step)
    Let E be an empty array
    foreach $x \in X_{K_d}^d$ **do**
        Consider the adjacent points to x given by $c, d \in I_{M_d}^d$ such that $c < x < d$
        $\lambda = Brent(c, d)$
        Append λ to E
    return $\underline{E}$

Remark 4.3.3. *Although the algorithm above was enough, we point some problems and possible changes to consider. First, there are no guarantees regarding the eigenvalues found: this depends on the chosen interval and on the step. For example, if the first eigenvalue is not in the chosen interval, it will never be found. One may also find a "jump" if two eigenvalues are arbitrarily close but the algorithm just found one of them: this is the case when an eigenvalue has multiplicity bigger than one, which depends on the domain. However, this last case is easy to spot if one considers the one parameter transformation between the domain Ω and the unitary disk $\mathbb{D}$ given by*

$$\Omega(t) = (1 - t)\mathbb{D} + t\Omega, \; t \in (0, 1),$$

*since the graph of the eigenvalues is continuous in respect to t. Regarding the complexity of the algorithm, the objective is to evaluate the function $\sigma_N(k)$ the least amount of time: a brute-force approach with a very small step is not feasible since each evaluation takes some time for big complex valued matrices. However, we note that the algorithm can be improved by just considering the initial point a and "walking forward" with step size h. In that case, one could bracket each local minimum individually and only leaving to the main loop when the maximum depth was reached for each local minimum initially found. The loop would **break** when the number of eigenvalues found attains a prescribed value.*

Before introducing a new technique to improve the condition of the system, we state a posteriori estimate based on a result proved by Moler and Payne in [54].

Theorem 4.3.4. *Let $\tilde{k}$ and $\tilde{u} \in C^2(\Omega) \cap C(\overline{\Omega})$ be an approximate eigenfrequency and eigenfunction which satisfy the following problem:*

$$\begin{cases} -\Delta\tilde{u} = k^2 u, & \text{in } \Omega \\ u = \xi(x), & \text{on } \Gamma. \end{cases}$$

Then, there exists an eigenfrequency k_n of (4.8) such that

$$\frac{\left|k_n - \tilde{k}\right|}{|k_n|} \le \theta$$

where

$$\theta = \frac{\sqrt{|\Omega|}\|\xi\|_{L^\infty(\Gamma)}}{\|\tilde{u}\|_{L^2(\Omega)}}.$$

If, in addition, $\tilde{u}_{L^2(\Omega)}$ and u is the normalized orthogonal projection of $\tilde{u}$ onto the eigenspace of k_n, then

$$\|\tilde{u} - u\|_{L^2(\Omega)} \le \frac{\theta}{\rho_n}\left(1 + \frac{\theta^2}{\rho_n^2}\right)^{\frac{1}{2}},$$

where

$$\rho_n = \min_{k_n \ne k_p} \frac{\left|k_p^2 - \tilde{k}^2\right|}{k_p^2}, \text{ for } p \in \mathbb{N}.$$

4.3.1 The Subspace Angle Technique

As stated before, one of the drawbacks of this method is the ill-conditioning of the system. In this subsection we introduce the so-called *Subspace Angle Technique*, first presented in [55]. Intuitively, there are two problems at play: firstly, while the MFS only needs the boundary data to approximate the solution of the BVP, the exponential growth of the condition number against the exponential convergence can be seen has the lack of information given by the collocation points on the boundary, which is not enough to decide if an approximate eigenfunction is spurious; secondly, while we proved the linear inde-

pendence of the basis functions, in practice the columns of the matrix $A(k)$ are almost linear dependent if its number is too large (in fact, this is, once again, associated with the distance from the boundary to the artificial boundary).

To solve the first problem, we add additional interior points in order to over determine the system; and for the second problem we construct an orthonormal basis of the column space of $A(k)$, denoted by $\mathcal{C}(A(k))$, using the QR factorization of $A(k)$. Let M_B be the number of boundary points and M_I the number of interior points, such that $M = M_B + M_I$. Then, by adding some interior points the matrix $A(k)$ can be extended to

$$A(k) = \begin{bmatrix} A_B(k) \\ A_I(k) \end{bmatrix},$$

where the indices B and I correspond to the block matrices with the boundary and interior collocation points, respectively. To generate an orthonormal basis of the column space of $A(k)$, consider the QR factorization of $A(k)$, given by $A(k) = Q(k)R$, where $Q(k)$ is a unitary complex matrix (i.e., $Q^\dagger(k) = Q^{-1}(k)$) and R is an upper triangular matrix. By partitioning $Q(k)$ in the boundary and interior collocation points we also have

$$Q(k) = \begin{bmatrix} Q_B(k) \\ Q_I(k) \end{bmatrix},$$

and each unit vector $u \in \mathcal{C}(A(k))$ has the form

$$u = \begin{bmatrix} u_B \\ u_I \end{bmatrix} = Q(k)v = \begin{bmatrix} Q_B(k) \\ Q_I(k) \end{bmatrix} v \tag{4.9}$$

for some $v \in \mathbb{R}^2$, $\|v\| = 1$. Assuming homogeneous Dirichlet boundary conditions, we are interested in non-trivial solutions $v \in \mathbb{R}^2$ to the above problem when $u \approx 0$ at the boundary, i.e, to solve the constrained minimization problem

$$\min_{v \in \mathbb{R}^2, \|v\|=1} \|Q_B(k)v\|.$$

The above problem is easy to solve and has a closed form solution which can be found using Lagrange multipliers. The solution $\check{v}$ is the right singular vector associated with the smallest singular value σ_N and

$$\sigma_N(k) = \|Q_B(k)\check{v}\|.$$

Let $\check{u} = Q(k)\check{v}$. Taking the norm on both sides of equation (4.9), one can write

$$1 = \|\check{u}\|^2 = \left\| \begin{bmatrix} Q_B(k) \\ Q_I(k) \end{bmatrix} \check{v} \right\|^2 = \sigma_N^2(k) + \|Q_I(k)\check{v}\|^2. \tag{4.10}$$

Notice how equation (4.10) can be used to eliminate spurious solutions: since $0 < \sigma_N < 1$, if $\sigma_N \approx 1$, then $Q_I(k)\check{v} \approx 0 \implies u_I \approx 0$ which is an incorrect solution (is zero on the interior and does not satisfy the boundary constraints); on the other hand, if $\sigma_N \approx 0$, then we found an eigenfunction which is small

on the boundary points and whose interior is not null.

The name Subspace Angle Technique comes from the fact that σ_N is related with the angle between the subspaces $\mathcal{C}(A(k))$ and $\mathcal{G}_0$, the space of vectors that are zero at boundary points[2]. The angle $\phi(k) = \angle(\mathcal{C}(A(k)), \mathcal{G}_0)$ between both subspaces is defined by

$$\cos \phi(k) = \sup_{\substack{u \in \mathcal{C}(A(k)),\, \|u\|=1 \\ v \in \mathcal{G}_0,\, \|v\|=1}} (u, v),$$

and one can prove (c.f. [55]) that

$$\sigma_N = \sin \phi(k).$$

Therefore, the discrete problem has a non-trivial solution (i.e. λ is an eigenvalue of the Laplace Operator) if and only if $\mathcal{C}(A(k))$ and $\mathcal{G}_0$ have a non-trivial intersection (i.e. $\phi(k) = l\pi$, $l \in \mathbb{Z}$).

Remark 4.3.5. *While the construction above assumed homogeneous Dirichlet boundary conditions, it can be easily generalized to any type of homogeneous boundary conditions $\mathcal{B}$ by considering the appropriate A matrix.*

Remark 4.3.6. *Neither the enrichment technique nor the Subspace Angle Technique are specific methods only applicable to the Laplace equation and the Helmholtz equation, respectively. They can be used for both equations and at the same time. For example, in [56], both methods were used to study the spectrum of the Laplace operator in domains with corners and cracks.*

---

[2]$\mathcal{G}_0$ can be seen as the discretization of the functions which satisfy the boundary conditions but not the Helmholtz equation.

<div style="text-align: right;">

5

</div>

Conducted Numerical Simulations

Contents

Thinks to do:

1. Dirac

   (a) Result against the ball with m=0 (accuracy)

   (b) Results for quadrilaterals and Conjecture

   (c) Results for triangles and Conjecture

   (d) Results for smooth domains

   (e) Third eigenvalue method

2. Transmission

   (a) (WE STILL NEED PROOF!)

   (b) Results against known function

   (c) Results for rectangle

   (d) Results for L + particular solutions

   (e) Results for smooth domains

5.1 Dirac equation simulations

5.2 Transmission problem simulations

For the Transmission problem, we now consider the set of equations studied previously in the subchapter 3.3, given by

$$
\begin{aligned}
-\nabla k_i \nabla u_i &= f_i, \text{ in } \Omega_i \\
u_1 - u_2 &= 0, \text{ on } \gamma \\
k_1 \frac{\partial u_1}{\partial n_1} + k_2 \frac{\partial u_2}{\partial n_2} &= 0, \text{ on } \gamma \\
u_i &= 0, \text{ on } \Gamma_i.
\end{aligned}
\tag{5.1}
$$

Like before, the domain $\Omega \subset \mathbb{R}^2$ is divided into two non-overlapping regions Ω_1 and Ω_2 such that $\overline{\Omega} = \overline{\Omega_1} \cup \overline{\Omega_2}$. Their common boundary is denoted by $\gamma = \partial\Omega_1 \cap \partial\Omega_2$ and the boundary of each domain (minus the common boundary) is also denoted by $\Gamma_i = \partial\Omega_1 \setminus \gamma$. In what follows, the source functions f_i of each domain are constant[1], and we took $f_i = 1$. Recall that $k_1 \geq k_2 > 0$ are constants and n_i is the

---

[1]In this work we only considered $f_i = 1$. In any case, we are still working with a general discontinuous source function (if $k_1 \neq k_2$). Working with different *continuous* source functions should make no difference in the result. We will also present how to deal with general and continuous source functions.

(normalized) outward normal to each domain subdomain $\Omega_i, i = 1, 2$, where we shall write $n = n_1 = -n_2$ when we are restricted to the interface.

The procedure presented here is based on [47] and [57]. Given that $f_i = 1$ for each $i = 1, 2$, a solution of (5.1) can be found by taking the following steps:

1. Find a solution for the non-homogeneous problem

$$\begin{cases} -\Delta u_1^{NH} = \frac{1}{k_1} \\ -\Delta u_2^{NH} = \frac{1}{k_2}. \end{cases}$$

   This can easily be done, and we have

$$\begin{cases} u_1^{NH} = -\frac{x_1^2 + x_2^2}{4k_1} \\ u_2^{NH} = -\frac{x_1^2 + x_2^2}{4k_2}; \end{cases}$$

2. Then we solve the homogeneous problem

$$-\nabla k_i \nabla u_i^H = 0, \text{ in } \Omega_i$$
$$u_1^H - u_2^H = u_2^{NH} - u_1^{NH}, \text{ on } \gamma$$
$$k_1 \frac{\partial u_1}{\partial n_1} + k_2 \frac{\partial u_2}{\partial n_2} = u_2^{NH} - u_1^{NH}, \text{ on } \gamma \qquad (5.2)$$
$$u_i = -u_i^{NH}, \text{ on } \Gamma_i;$$

3. Finally, the solution of (5.1) is $u_i = u_i^H + u_i^{NH}$.

For general source functions, the steps above can also be used: however, it may not be possible to find an analytical solution in first step. In this case, **1.** must be solved numerically. A popular choice is to use radial basis functions (RBFs) (see [58] for example), like the thin plate spline

$$\varphi(r) = r^2 \log r,$$

and find the coefficients α_j in $f_i(x_k) = \tilde{f}_i(x_k) = \sum_{j=1}^n \alpha_j \varphi_j(x_k)$ using least square methods, where x_k are collocation points. Finally, one can analytically solve the equation $-\Delta \Psi_j = \varphi_j$ to recover the non-homogeneous solutions u_1^{NH} and u_2^{NH}. In [47] and [57] a different approach was suggested using the fundamental solutions of the Helmholtz equation instead of the classical RBFs; that method is known today as *Kansa MFS method*.

In what follows, the numerical results illustrate the accuracy of the method in simply connected 2D domains. Let N_i denote the number of source points for each domain i, such that $N = N_1 + N_2$. We denote the approximate solution by

$$\tilde{u} = \begin{cases} \tilde{u}_1, & \text{in } \Omega_1 \\ \tilde{u}_2, & \text{in } \Omega_2, \end{cases}$$

where

$$\tilde{u}_1(x) = \sum_{j=1}^{N_1} \alpha_j^{(1)} \Phi\left(x - y_j^{(1)}\right)$$

$$\tilde{u}_2(x) = \sum_{j=1}^{N_2} \alpha_j^{(2)} \Phi\left(x - y_j^{(1)}\right).$$

Let M_i be the number of boundary collocation points $x_m^{(i)}$ for each Ω_i and $M = M_1 + M_2$. We also consider Q interface points $z_q \in \gamma$ with $q = 1, \ldots, Q$. Then, a full block system is written as

$$\begin{bmatrix} \left[\Phi\left(x_m^{(1)} - y_j^{(1)}\right)\right] & [0] \\ [0] & \left[\Phi\left(x_m^{(2)} - y_j^{(2)}\right)\right] \\ \left[\Phi\left(z_q - y_j^{(1)}\right)\right] & \left[-\Phi\left(z_q - y_j^{(2)}\right)\right] \\ \left[k_1 \partial_n \Phi\left(z_q - y_j^{(1)}\right)\right] & \left[-k_2 \partial_n \Phi\left(z_q - y_j^{(2)}\right)\right] \end{bmatrix} \begin{bmatrix} \left[\alpha_j^{(1)}\right] \\ \left[\alpha_j^{(2)}\right] \end{bmatrix} = \begin{bmatrix} \left[-u_1^{NH}(x_m^{(1)})\right] \\ \left[-u_2^{NH}(x_m^{(2)})\right] \\ \left[u_2^{NH}(z_q) - u_1^{NH}(z_q)\right] \\ \left[k_2 \partial_n u_2^{NH}(z_q) - k_1 \partial_n u_1^{NH}(z_q)\right] \end{bmatrix} \quad (5.3)$$

Most of the examples below do not have analytical solution: only in the subsection 5.2.1, when we test the results against a known solution, we are able to find the absolute error. In the other cases we are only interested in the relative error, i.e, the boundary error (against which we can compare since $u_i = 0$ in Γ_i) and the interface error by checking the transmission conditions on γ:

- $\|\tilde{u}_i - 0\|_{L^2(\Gamma_i)}$, $i = 1, 2$: boundary collocation error;

- $\|\tilde{u}_1 - \tilde{u}_2\|_{L^2(\gamma)}$, $i = 1, 2$: continuity error (C^0) of $\tilde{u}$ across γ;

- $\|k_1 \partial_n \tilde{u}_1 - k_2 \partial_n \tilde{u}_2\|_{L^2(\gamma)}$, $i = 1, 2$: continuity error C^1 of $\partial_n \tilde{u}$ across γ.

From a numerical point of view, let $\mathcal{I}$ be the sample of test points. The L^2 norm is discretized into the Root Mean Squared Error (RMSE) which is equivalent to the l^2 norm and is given by

$$\|u - \tilde{u}\| = \sqrt{\frac{1}{\#\mathcal{I}} \sum_{z \in \mathcal{I}} |u(z) - \tilde{u}(z)|^2}.$$

For every result below the number of sample test points is 5 times larger than the sample used to find the coefficients of the MFS.

5.2.1 Numerical validation of the method

First, we start by testing the numerical algorithm for the unit disk $\mathbb{D}$, with $k_1 = k_2 = 1$. From Theorem (3.3.3), we know that the system of differential equations (5.1) is equivalent to the Poisson equation

$$-\Delta u = 1, \text{ in } \mathbb{D}$$
$$u = 0, \text{ on } \partial\mathbb{D}, \tag{5.4}$$

and is easy so see that the exact solution of Equation (5.4) is given in polar coordinates by $u(r, \theta) = \frac{1-r^2}{4}$.
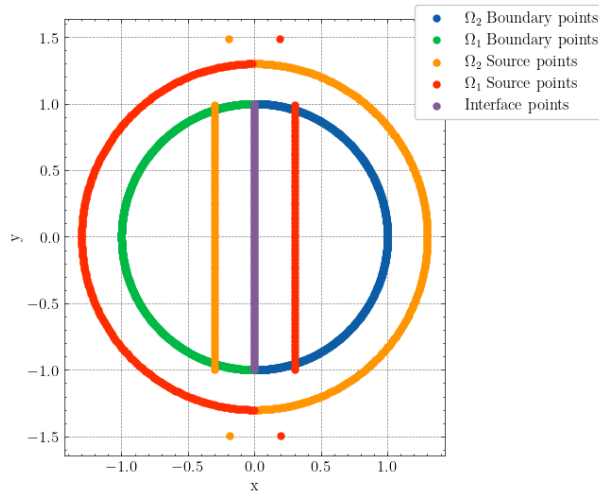

Figure 5.1: Configuration of the boundary, source and interface points. Each domain has 600 boundary points, 377 source points and the common interface has 100 points.
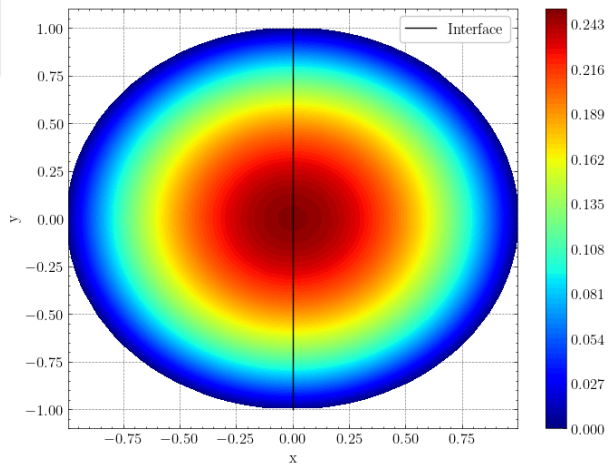
Figure 5.2: Numerical approximation of the BVP (5.4) under the conditions presented in Figure 5.1

The absolute error between the approximate solution and the exact solution can then be calculated for each domain point. The sample points to compute the absolute error were generated in a uniform grid and were also used to plot Figure 5.2. The method described at the end of the subchapter 4.1 was used to place the source points, where $\eta = 0.3$.

Boundary/Interface Points	Boundary Error		Absolute Error	
	Domain 1	Domain 2	Domain 1	Domain 2
600/150	9.759×10^{-12}	9.541×10^{-12}	1.465×10^{-11}	1.439×10^{-11}
500/100	3.667×10^{-11}	3.945×10^{-11}	9.382×10^{-11}	9.310×10^{-11}
412/100	3.721×10^{-11}	5.036×10^{-11}	9.652×10^{-11}	9.584×10^{-11}

Table 5.1: Numerical errors for the boundary and the whole Domains Ω_1 and Ω_2

The numerical results presented in Tables 5.1 and 5.2 are not yet optimal. When considering a larger value of η, the results increase by more than two orders of magnitude, but this also leads to a significant

Boundary/Interface Points	Interface C^0 Error	Interface C^1 Error	Condition number
600/150	6.945×10^{-11}	1.841×10^{-11}	2.528×10^{19}
500/100	3.910×10^{-10}	1.100×10^{-10}	2.382×10^{18}
412/100	4.035×10^{-10}	1.342×10^{-10}	7.597×10^{17}

Table 5.2: Numerical error on the interface γ. The condition number of the matrix is also presented.

increase in the already very high condition number (see Table 5.2), as expected. Despite this, the results show great promise, which was anticipated due to the analyticity of the domain.

As mentioned previously, the Method of Fundamental Solutions (MFS) yields better results in highly regular domains, even when considering curved geometries. However, increasing the number of boundary and interface collocation points improves the accuracy of the solution. It is important to note that a larger number of points also escalates the condition number, making the problem more challenging to solve accurately.

The inclusion of the "corner" source points, as depicted in Figure 5.1, also significantly impacts the method's accuracy. These source points above and below the interface (5.1) are strategically added, in order to capture the behavior near the interface corner. In Figure 5.1, observe that the source points for one of the domains can be inside the other domain, as the solution will be split into two parts.

5.2.2   Results for the rectangle

In this subsection a rectangular domain $[-1, -0.5] \times [1, 0.5]$ with a vertical interface along the line $x = 0$ is considered. We are now interested to study the problem for $k_1 \neq k_2$ where $k_2 = 1$ is fixed. The results below were conducted with 600 boundary points and 404 source points for each domain. The number of interface points is 150 and $\eta = 0.08$.

k_1 **value**	**Boundary Error**		**Interface Errors**		**Condition number**
	Domain 1	**Domain 2**	C^0	C^1	
1	7.775×10^{-8}	7.779×10^{-8}	4.732×10^{-9}	7.589×10^{-9}	2.331×10^{13}
2	4.398×10^{-8}	8.614×10^{-8}	2.499×10^{-6}	7.868×10^{-8}	3.623×10^{13}
3	2.181×10^{-8}	1.036×10^{-7}	3.838×10^{-6}	1.551×10^{-7}	8.182×10^{13}

Table 5.3: Numerical error on the interface γ. The condition number of the matrix is also presented.

In Figures 5.3, 5.4 and 5.5 we present the numerical approximation for different k_1 values. Observe that increasing k_1 breaks the symmetry of the solution which shifts from Ω_1 (the domain on the left) and Ω_2 (the domain on the right). Table 5.3 summarizes the results for different k_1 values. While the results are slightly worst that the previous ones due to the worst domain regularity, they still preserve high accuracy. It is worth to remark that for different values of k_1 and k_2 decreases the accuracy of the method. This is also to be expected, since we are dealing with a discontinuous source function which
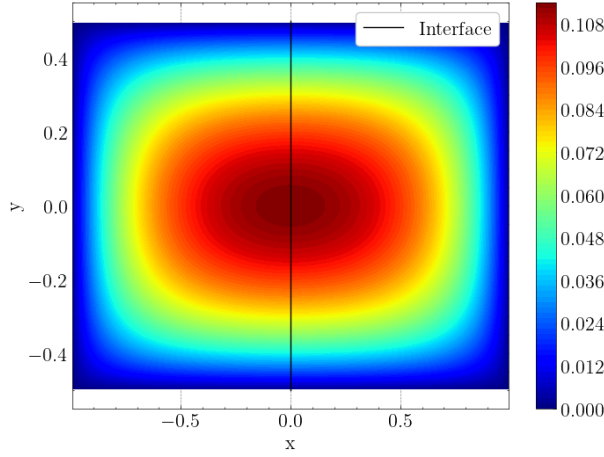
Figure 5.3: Numerical simulation with $k_1 = 1$.
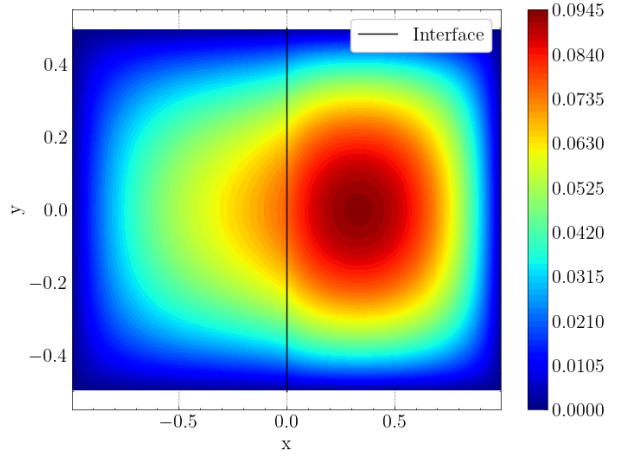
Figure 5.4: Numerical simulation with $k_1 = 2$.
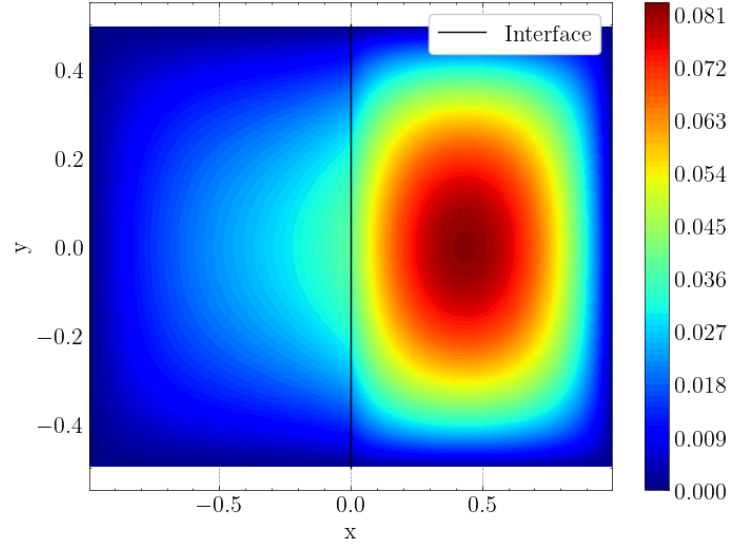
Figure 5.5: Numerical simulation with $k_1 = 5$.

Numerical approximations of the BVP for a rectangular domain with different k_1 values.

decreases the regularity of the solution.

Notice that the condition number for the rectangle is smaller than the one presented in Table 5.2 for the unit disk. This is a consequence of a smaller value of η, which in this case appears to be optimal, since increasing its value decreases the overall accuracy.

5.2.3   Results for an L-shape domain with enrichment

In the previous subsection a domain with corners was analyzed. However, it still preserved some regularity and the MFS with classical basis functions was able to capture its corner's behavior, as explained

in Remark 4.2.3. In what follows, we are going to study the case of an L-shape, a non-convex domain with singular corners. Two different interfaces will be considered: first, the usual interface along the line $x = 0$; then, along its symmetry axis with the line $y = \frac{1}{2}x$.

Consider the L-shape given in Figure 5.6. The left and the right subdomains are Ω_1 and Ω_2, respectively. Again, the number of interface points is 150 and the number of source points for each domain is 428. The number of boundary collocation points for Ω_1 and Ω_2 are 710 and 639, respectively.
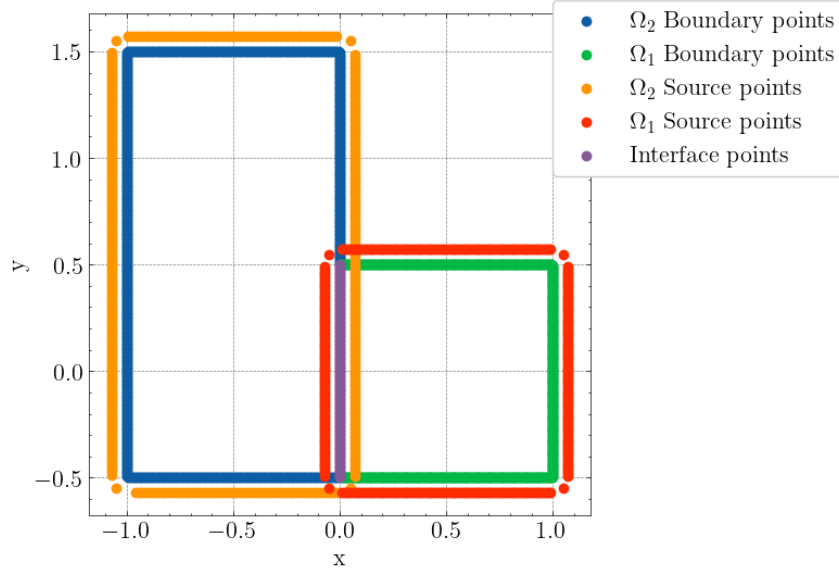

Figure 5.6: L-shape domain with vertical interface. Configuration of the boundary, source and interface points.

5.2.4 Results for the smooth domains

6

Conclusion

Contents

Pellentesque vel dui sed orci faucibus iaculis. Suspendisse dictum magna id purus tincidunt rutrum. Nulla congue. Vivamus sit amet lorem posuere dui vulputate ornare. Phasellus mattis sollicitudin ligula. Duis dignissim felis et urna. Integer adipiscing congue metus.

6.1   Conclusions

Lorem ipsum dolor sit amet, consectetuer adipiscing elit. Morbi commodo, ipsum sed pharetra gravida, orci magna rhoncus neque, id pulvinar odio lorem non turpis. Nullam sit amet enim. Suspendisse id velit vitae ligula volutpat condimentum. Aliquam erat volutpat. Sed quis velit. Nulla facilisi. Nulla libero. Vivamus pharetra posuere sapien. Nam consectetuer. Sed aliquam, nunc eget euismod ullamcorper, lectus nunc ullamcorper orci, fermentum bibendum enim nibh eget ipsum. Donec porttitor ligula eu dolor. Maecenas vitae nulla consequat libero cursus venenatis. Nam magna enim, accumsan eu, blandit sed, blandit a, eros.

Quisque facilisis erat a dui. Nam malesuada ornare dolor. Cras gravida, diam sit amet rhoncus ornare, erat elit consectetuer erat, id egestas pede nibh eget odio. Proin tincidunt, velit vel porta elementum, magna diam molestie sapien, non aliquet massa pede eu diam. Aliquam iaculis. Fusce et ipsum et nulla tristique facilisis. Donec eget sem sit amet ligula viverra gravida. Etiam vehicula urna vel turpis. Suspendisse sagittis ante a urna. Morbi a est quis orci consequat rutrum. Nullam egestas feugiat felis. Integer adipiscing semper ligula. Nunc molestie, nisl sit amet cursus convallis, sapien lectus pretium metus, vitae pretium enim wisi id lectus. Donec vestibulum. Etiam vel nibh. Nulla facilisi. Mauris pharetra. Donec augue. Fusce ultrices, neque id dignissim ultrices, tellus mauris dictum elit, vel lacinia enim metus eu nunc.

Proin at eros non eros adipiscing mollis. Donec semper turpis sed diam. Sed consequat ligula nec tortor. Integer eget sem. Ut vitae enim eu est vehicula gravida. Morbi ipsum ipsum, porta nec, tempor id, auctor vitae, purus. Pellentesque neque. Nulla luctus erat vitae libero. Integer nec enim. Phasellus aliquam enim et tortor. Quisque aliquet, quam elementum condimentum feugiat, tellus odio consectetuer wisi, vel nonummy sem neque in elit. Curabitur eleifend wisi iaculis ipsum. Pellentesque habitant morbi tristique senectus et netus et malesuada fames ac turpis egestas. In non velit non ligula laoreet ultrices. Praesent ultricies facilisis nisl. Vivamus luctus elit sit amet mi. Phasellus pellentesque, erat eget elementum volutpat, dolor nisl porta neque, vitae sodales ipsum nibh in ligula. Maecenas mattis pulvinar diam. Curabitur sed leo.

Nulla facilisi. In vel sem. Morbi id urna in diam dignissim feugiat. Proin molestie tortor eu velit. Aliquam erat volutpat. Nullam ultrices, diam tempus vulputate egestas, eros pede varius leo, sed imperdiet lectus est ornare odio. Lorem ipsum dolor sit amet, consectetuer adipiscing elit. Proin consectetuer velit in dui. Phasellus wisi purus, interdum vitae, rutrum accumsan, viverra in, velit. Sed enim risus, congue

non, tristique in, commodo eu, metus. Aenean tortor mi, imperdiet id, gravida eu, posuere eu, felis. Mauris sollicitudin, turpis in hendrerit sodales, lectus ipsum pellentesque ligula, sit amet scelerisque urna nibh ut arcu. Aliquam in lacus. Vestibulum ante ipsum primis in faucibus orci luctus et ultrices posuere cubilia Curae; Nulla placerat aliquam wisi. Mauris viverra odio. Quisque fermentum pulvinar odio. Proin posuere est vitae ligula. Etiam euismod. Cras a eros.

Nunc auctor bibendum eros. Maecenas porta accumsan mauris. Etiam enim enim, elementum sed, bibendum quis, rhoncus non, metus. Fusce neque dolor, adipiscing sed, consectetuer et, lacinia sit amet, quam.

6.2   System Limitations and Future Work

Aliquam aliquet, est a ullamcorper condimentum, tellus nulla fringilla elit, a iaculis nulla turpis sed wisi. Fusce volutpat. Etiam sodales ante id nunc. Proin ornare dignissim lacus. Nunc porttitor nunc a sem. Sed sollicitudin velit eu magna. Aliquam erat volutpat. Vivamus ornare est non wisi. Proin vel quam. Vivamus egestas. Nunc tempor diam vehicula mauris. Nullam sapien eros, facilisis vel, eleifend non, auctor dapibus, pede.

Bibliography

[1] Z.-C. Li and T.-T. Lu, "Singularities and treatments of elliptic boundary value problems," *Mathematical and Computer Modelling*, vol. 31, no. 8-9, pp. 97–145, 2000.

[2] W. Rudin, *Functional Analysis*, ser. International series in pure and applied mathematics. McGraw-Hill, 1991. [Online]. Available: https://books.google.pt/books?id=Sh_vAAAAMAAJ

[3] H. Brezis and H. Brézis, *Functional analysis, Sobolev spaces and partial differential equations*. Springer, 2011, vol. 2, no. 3.

[4] W. Arendt and K. Urban, *Partielle differenzialgleichungen*. Springer, 2010.

[5] J. L. Lions and E. Magenes, *Non-homogeneous boundary value problems and applications: Vol. 1*. Springer Science & Business Media, 2012, vol. 181.

[6] H. Tavares, "Partial differential equations, lecture notes," https://ulisboa-my.sharepoint.com/:b:/g/personal/ist27898_tecnico_ulisboa_pt/EfizUpSVmCRCo0Nst2a-sacBDwFrkPuh9w8A55EU9BoFmA?e=kY5B2R.

[7] L. C. Evans, *Partial differential equations*. American Mathematical Society, 2022, vol. 19.

[8] A. Bogomolny, "Fundamental solutions method for elliptic boundary value problems," *SIAM Journal on Numerical Analysis*, vol. 22, no. 4, pp. 644–669, 1985.

[9] S. N. Chandler-Wilde, D. P. Hewett, and A. Moiola, "Sobolev spaces on non-lipschitz subsets of r n with application to boundary integral equations on fractal screens," *Integral Equations and Operator Theory*, vol. 87, no. 2, pp. 179–224, 2017.

[10] D. P. Hewett and A. Moiola, "A note on properties of the restriction operator on sobolev spaces," *Journal of Applied Analysis*, vol. 23, no. 1, pp. 1–8, 2017.

[11] G. Geymonat, "Trace theorems for sobolev spaces on lipschitz domains. necessary conditions," in *Annales mathématiques Blaise Pascal*, vol. 14, no. 2, 2007, pp. 187–197.

[12] J. Necas, *Direct methods in the theory of elliptic equations.* Springer Science & Business Media, 2011.

[13] G. Chen and J. Zhou, *Boundary element methods with applications to nonlinear problems.* Springer Science & Business Media, 2010, vol. 7.

[14] L. Hörmander, *The analysis of linear partial differential operators I: Distribution theory and Fourier analysis.* Springer, 2015.

[15] L. C. Evans and R. F. Gariepy, *Measure theory and fine properties of functions.* CRC press, 2015.

[16] R. Courant and D. Hilbert, *Methods of mathematical physics: partial differential equations.* John Wiley & Sons, 2008.

[17] D. Borthwick, *Spectral Theory: Basic Concepts and Applications.* Springer Nature, 2020, vol. 284.

[18] M. Reed and B. Simon, *II: Fourier Analysis, Self-Adjointness.* Elsevier, 1975, vol. 2.

[19] A. Henrot, *Extremum problems for eigenvalues of elliptic operators.* Springer Science & Business Media, 2006.

[20] ——, *Shape optimization and spectral theory.* De Gruyter Open, 2017.

[21] E. Krahn, "Über minimaleigenschaften der kugel in drei und mehr dimensionen," *(No Title)*, 1926.

[22] P. Freitas and D. Krejčiřík, "A sharp upper bound for the first dirichlet eigenvalue and the growth of the isoperimetric constant of convex domains," *Proceedings of the American Mathematical Society*, vol. 136, no. 8, pp. 2997–3006, 2008.

[23] S. A. Wolf and J. B. Keller, "Range of the first two eigenvalues of the laplacian," *Proceedings of the Royal Society of London. Series A: Mathematical and Physical Sciences*, vol. 447, no. 1930, pp. 397–412, 1994.

[24] A. Henrot and D. Bucur, "Minimization of the third eigenvalue of the dirichlet laplacian," *Proceedings of the Royal Society of London. Series A: Mathematical, Physical and Engineering Sciences*, vol. 456, no. 1996, pp. 985–996, 2000.

[25] D. Bucur, "Minimization of the k-th eigenvalue of the dirichlet laplacian," *Archive for Rational Mechanics and Analysis*, vol. 206, no. 3, pp. 1073–1083, 2012.

[26] D. Mazzoleni and A. Pratelli, "Existence of minimizers for spectral problems," *Journal de Mathématiques Pures et Appliquées*, vol. 100, no. 3, pp. 433–453, 2013.

[27] G. Pólya and G. Szegö, *Isoperimetric inequalities in mathematical physics.* Princeton University Press, 1951, no. 27.

[28] B. Bogosel and D. Bucur, "On the polygonal faber-krahn inequality," *arXiv preprint arXiv:2203.16409*, 2022.

[29] J. Gómez-Serrano and G. Orriols, "Any three eigenvalues do not determine a triangle," *Journal of Differential Equations*, vol. 275, pp. 920–938, 2021.

[30] P. R. Antunes and P. Freitas, "On the inverse spectral problem for euclidean triangles," *Proceedings of the Royal Society A: Mathematical, Physical and Engineering Sciences*, vol. 467, no. 2130, pp. 1546–1562, 2011.

[31] M. Kac, "Can one hear the shape of a drum?" *The american mathematical monthly*, vol. 73, no. 4P2, pp. 1–23, 1966.

[32] C. Gordon, D. Webb, and S. Wolpert, "Isospectral plane domains and surfaces via riemannian orbifolds," *Inventiones mathematicae*, vol. 110, no. 1, pp. 1–22, 1992.

[33] P. A. M. Dirac, "The quantum theory of the electron," *Proceedings of the Royal Society of London. Series A, Containing Papers of a Mathematical and Physical Character*, vol. 117, no. 778, pp. 610–624, 1928.

[34] P. Briet and D. Krejčiřík, "Spectral optimization of dirac rectangles," *Journal of Mathematical Physics*, vol. 63, no. 1, p. 013502, 2022.

[35] T. Vu, "Spectral inequality for dirac right triangles," *arXiv preprint arXiv:2302.13040*, 2023.

[36] D. Krejcirik, S. Larson, and V. Lotoreichik, "Problem list of the aim workshop," 2019. [Online]. Available: http://aimpl.org/shapesurface/

[37] R. D. Benguria, S. Fournais, E. Stockmeyer, and H. Van Den Bosch, "Spectral gaps of dirac operators describing graphene quantum dots," *Mathematical Physics, Analysis and Geometry*, vol. 20, pp. 1–12, 2017.

[38] V. Lotoreichik and T. Ourmières-Bonafos, "A sharp upper bound on the spectral gap for graphene quantum dots," *Mathematical Physics, Analysis and Geometry*, vol. 22, pp. 1–30, 2019.

[39] A. Quarteroni and A. Valli, *Domain decomposition methods for partial differential equations*. Oxford University Press, 1999, no. BOOK.

[40] R. A. Adams and J. J. Fournier, *Sobolev spaces*. Elsevier, 2003.

[41] C. J. Alves, "On the choice of source points in the method of fundamental solutions," *Engineering Analysis with Boundary Elements*, vol. 33, no. 12, pp. 1348–1361, 2009.

[42] R. Narasimhan and Y. Nievergelt, *Complex analysis in one variable*. Springer Science & Business Media, 2012.

[43] R. Kress, *Linear Integral Equations*, ser. Applied Mathematical Sciences. Springer New York, 2013.

[44] D. Colton and R. Kress, *Integral equation methods in scattering theory*. SIAM, 2013.

[45] S. Salsa, *Partial differential equations in action: from modelling to theory*. Springer, 2016, vol. 99.

[46] S. Valtchev, "Numerical analysis of methods with fundamental solutions for acoustic and elastic wave propagation problems," Ph.D. dissertation, Universidade Técnica de Lisboa, Instituto Superior Técnico, 2008.

[47] C. Alves and C. Chen, "A new method of fundamental solutions applied to nonhomogeneous elliptic problems," *Advances in Computational Mathematics*, vol. 23, pp. 125–142, 2005.

[48] S. Christiansen and E. Meister, "Condition number of matrices derived from two classes of integral equations," *Mathematical Methods in the Applied Sciences*, vol. 3, no. 1, pp. 364–392, 1981.

[49] T. Kitagawa, "On the numerical stability of the method of fundamental solution applied to the dirichlet problem," *Japan Journal of Applied Mathematics*, vol. 5, pp. 123–133, 1988.

[50] ——, "Asymptotic stability of the fundamental solution method," *Journal of Computational and Applied Mathematics*, vol. 38, no. 1-3, pp. 263–269, 1991.

[51] A. H. Barnett and T. Betcke, "Stability and convergence of the method of fundamental solutions for helmholtz problems on analytic domains," *Journal of Computational Physics*, vol. 227, no. 14, pp. 7003–7026, 2008.

[52] C. J. Alves and P. R. Antunes, "The method of fundamental solutions applied to the calculation of eigenfrequencies and eigenmodes of 2d simply connected shapes," *CMC-TECH SCIENCE PRESS*-, vol. 2, no. 4, p. 251, 2005.

[53] R. P. Brent, "An algorithm with guaranteed convergence for finding a zero of a function," *The computer journal*, vol. 14, no. 4, pp. 422–425, 1971.

[54] C. Moler and L. Payne, "Bounds for eigenvalues and eigenvectors of symmetric operators," *SIAM Journal on Numerical Analysis*, vol. 5, no. 1, pp. 64–70, 1968.

[55] T. Betcke and L. N. Trefethen, "Reviving the method of particular solutions," *SIAM review*, vol. 47, no. 3, pp. 469–491, 2005.

[56] P. R. Antunes and S. S. Valtchev, "A meshfree numerical method for acoustic wave propagation problems in planar domains with corners and cracks," *Journal of Computational and Applied Mathematics*, vol. 234, no. 9, pp. 2646–2662, 2010.

[57] C. J. Alves, N. F. Martins, and S. S. Valtchev, "Domain decomposition methods with fundamental solutions for helmholtz problems with discontinuous source terms," *Computers & Mathematics with Applications*, vol. 88, pp. 16–32, 2021.

[58] M. A. Golberg, C.-S. Chen, and S. Karur, "Improved multiquadric approximation for partial differential equations," *Engineering Analysis with boundary elements*, vol. 18, no. 1, pp. 9–17, 1996.

Glossary

This document is incomplete. The external file associated with the glossary 'main' (which should be called `main.gls`) hasn't been created.

Check the contents of the file `main.glo`. If it's empty, that means you haven't indexed any of your entries in this glossary (using commands like `\gls` or `\glsadd`) so this list can't be generated. If the file isn't empty, the document build process hasn't been completed.

If you don't want this glossary, add `nomain` to your package option list when you load `glossaries-extra.sty`. For example:

```
\usepackage[nomain]{glossaries-extra}
```

Try one of the following:

- Add `automake` to your package option list when you load `glossaries-extra.sty`. For example:

  ```
  \usepackage[automake]{glossaries-extra}
  ```

- Run the external (Lua) application:

  ```
  makeglossaries-lite.lua "main"
  ```

- Run the external (Perl) application:

  ```
  makeglossaries "main"
  ```

Then rerun LaTeX on this document.

This message will be removed once the problem has been fixed.

A

Code of Project

Nulla dui purus, eleifend vel, consequat non, dictum porta, nulla. Duis ante mi, laoreet ut, commodo eleifend, cursus nec, lorem. Aenean eu est. Etiam imperdiet turpis. Praesent nec augue. Curabitur ligula quam, rutrum id, tempor sed, consequat ac, dui. Vestibulum accumsan eros nec magna. Vestibulum vitae dui. Vestibulum nec ligula et lorem consequat ullamcorper.

Listagem A.1: Example of a XML file.

```xml
1  <?xml version="1.0" encoding="UTF-8"?>
2  <StreamInfo version="2.0">
3      <Clip duration="PT01M0.00S">
4          <BaseURL>videos/</BaseURL>
5          <Description>svc_1</Description>
6          <Representation mimeType="video/SVC" codecs="svc" frameRate="30.00" bandwidth="401.90"
7              width="176" height="144" id="L0">
8              <BaseURL>svc_1/</BaseURL>
9              <SegmentInfo from="0" to="11" duration="PT5.00S">
```

```
10          <BaseURL>svc_1-L0-</BaseURL>

11        </SegmentInfo>

12      </Representation>

13    <Representation mimeType="video/SVC" codecs="svc" frameRate="30.00" bandwidth="1322.60"

14        width="352" height="288" id="L1">

15      <BaseURL>svc_1/</BaseURL>

16      <SegmentInfo from="0" to="11" duration="PT5.00S">

17        <BaseURL>svc_1-L1-</BaseURL>

18      </SegmentInfo>

19    </Representation>

20  </Clip>

21 </StreamInfo>
```

Etiam imperdiet turpis. Praesent nec augue. Curabitur ligula quam, rutrum id, tempor sed, consequat ac, dui. Maecenas tincidunt velit quis orci. Sed in dui. Nullam ut mauris eu mi mollis luctus. Class aptent taciti sociosqu ad litora torquent per conubia nostra, per inceptos hymenaeos. Sed cursus cursus velit. Sed a massa. Duis dignissim euismod quam.

Listagem A.2: Assembler Main Code.

```
1  ; **********************************************************************
2  ; * Constantes
3  ; **********************************************************************
4
5  ON      EQU 1 ; contagem ligada
6  OFF     EQU 0 ; contagem desligada
7  INPUT EQU 8000H ; endereço do porto de entrada
8           ;(bit 0 = RTC; bit 1 = botão)
9  OUTPUT  EQU 8000H ; endereço do porto de saída.
10
11
12 ; **********************************************************************
13 ; * Stack
14 ; **********************************************************************
15
16 PLACE   1000H
17 pilha:    TABLE 100H  ; espaço reservado para a pilha
18 fim_pilha:
19
20
21 ; **********************************************************************
22 PLACE   2000H
23
24 ; Tabela de vectores de interrupção
25
26 tab:    WORD   rot0
27
28 ; **********************************************************************
29 ; * Programa Principal
30 ; **********************************************************************
31
32 PLACE   0
33
34 inicio:
35   MOV BTE, tab    ; incializa BTE
36   MOV R9, INPUT   ; endereço do porto de entrada
37   MOV R10, OUTPUT  ; endereço do porto de Ìsada
38   MOV SP, fim_pilha
39   MOV R5, 1     ; inicializa estado do processo P1
40   MOV R6, 1     ; inicializa estado do processo P2
41   MOV R4, OFF    ; inicializa controle de RTC
42   MOV R8, 0     ; inicializa contador
43   MOV R7, OFF    ; inicialmente não permite contagem
44   EIO           ; permite interrupções tipo 0
```

```asm
45    EI            ; activa interrupções
46
47  ciclo:
48    CALL  P1       ; invoca processo P1
49    CALL  P2       ; invoca processo P2
50    JMP   ciclo  ; repete ciclo
51
52  ; ************************************************************************
53  ;* ROTINAS
54  ; ************************************************************************
55
56  P1:
57    CMP R5, 1    ; se estado = 1
58    JZ  P1_1
59    CMP R5, 2    ; se estado = 2
60    JZ  P1_2
61  sai_P1:
62    RET          ; sai do processo.
63
64
65  P1_1:
66    MOVB  R0, [R9]  ; lê porto de entrada
67    BIT R0, 1
68    JZ  sai_P1    ; se botão não carregado, sai do processo
69    MOV R7, ON    ; permite contagem do display
70    MOV R5, 2   ; passa ao estado 2 do P1
71    JMP sai_P1
72
73  P1_2:
74    MOVB  R0, [R9]  ; lê porto de entrada
75    BIT R0, 1
76    JNZ sai_P1    ; se botão continua carregado, sai do processo
77    MOV R7, OFF   ; caso contrário, desliga contagem do display
78    MOV R5, 1   ; passa ao estado 1 do P1
79    JMP sai_P1
```

Class aptent taciti sociosqu ad litora torquent per conubia nostra, per inceptos hymenaeos. Phasellus eget nisl ut elit porta ullamcorper. Maecenas tincidunt velit quis orci. Sed in dui. Nullam ut mauris eu mi mollis luctus. Class aptent taciti sociosqu ad litora torquent per conubia nostra, per inceptos hymenaeos.

This inline MATLAB code `for i=1:3, disp('cool'); end;` uses the \mcode{} command.[1]

Nullam ut mauris eu mi mollis luctus. Class aptent taciti sociosqu ad litora torquent per conubia nostra, per inceptos hymenaeos. Sed cursus cursus velit. Sed a massa. Duis dignissim euismod quam. Nullam euismod metus ut orci.

Listagem A.3: `Matlab Function`

```matlab
1  for i = 1:3
2      if i >= 5 && a ~= b        % literate programming replacement
3          disp('cool');         % comment with some LaTeXin it:  πx²
4      end
5      [:,ind] = max(vec);
6      x_last = x(1,end) - 1;
7      v(end);
8      ylabel('Voltage (µV)');
9  end
```

---

[1]MATLAB Works also in footnotes: `for i=1:3, disp('cool'); end;`

Nullam ut mauris eu mi mollis luctus. Class aptent taciti sociosqu ad litora torquent per conubia nostra, per inceptos hymenaeos. Sed cursus cursus velit. Sed a massa. Duis dignissim euismod quam. Nullam euismod metus ut orci.

Listagem A.4: `function.m`

```matlab
1  %    Copyright 2010 The MathWorks, Inc.
2  function ObjTrack(position)
3  % #codegen
4  % First, setup the figure
5  numPts = 300;               % Process and plot 300 samples
6  figure;hold;grid;           % Prepare plot window
7  % Main loop
8  for idx = 1: numPts
9      z = position(:,idx);    % Get the input data
10     y = kalmanfilter(z);    % Call Kalman filter to estimate the position
11     plot_trajectory(z,y);   % Plot the results
12  end
13  hold;
14  end    % of the function
```

Class aptent taciti sociosqu ad litora torquent per conubia nostra, per inceptos hymenaeos. Phasellus eget nisl ut elit porta ullamcorper. Maecenas tincidunt velit quis orci. Sed in dui. Nullam ut mauris eu mi mollis luctus. Class aptent taciti sociosqu ad litora torquent per conubia nostra, per inceptos hymenaeos. Sed cursus cursus velit. Sed a massa. Duis dignissim euismod quam. Nullam euismod metus ut orci. Vestibulum erat libero, scelerisque et, porttitor et, varius a, leo.

Listagem A.5: HTML with CSS Code

```html
1  <!DOCTYPE html>
2  <html>
3    <head>
4      <title>Listings Style Test</title>
5      <meta charset="UTF-8">
6      <style>
7        /* CSS Test */
8        * {
9          padding: 0;
10         border: 0;
```

```
11          margin: 0;
12        }
13    </style>
14    <link rel="stylesheet" href="css/style.css" />
15  </head>
16  <header> hey </header>
17  <article> this is a article </article>
18  <body>
19    <!-- Paragraphs are fine -->
20    <div id="box">
21      <p>
22        Hello World
23      </p>
24      <p>Hello World</p>
25      <p id="test">Hello World</p>
26      <p></p>
27    </div>
28    <div>Test</div>
29    <!-- HTML script is not consistent -->
30    <script src="js/benchmark.js"></script>
31    <script>
32      function createSquare(x, y) {
33        // This is a comment.
34        var square = document.createElement('div');
35        square.style.width = square.style.height = '50px';
36        square.style.backgroundColor = 'blue';
37
38        /*
39         * This is another comment.
40         */
41        square.style.position = 'absolute';
42        square.style.left = x + 'px';
43        square.style.top = y + 'px';
44
45        var body = document.getElementsByTagName('body')[0];
46        body.appendChild(square);
47      };
48
```

```
49        // Please take a look at +=
50        window.addEventListener('mousedown', function(event) {
51          // German umlaut test: Berührungspunkt ermitteln
52          var x = event.touches[0].pageX;
53          var y = event.touches[0].pageY;
54          var lookAtThis += 1;
55        });
56      </script>
57    </body>
58  </html>
```

Nulla dui purus, eleifend vel, consequat non, dictum porta, nulla. Duis ante mi, laoreet ut, commodo eleifend, cursus nec, lorem. Aenean eu est. Etiam imperdiet turpis. Praesent nec augue. Curabitur ligula quam, rutrum id, tempor sed, consequat ac, dui. Vestibulum accumsan eros nec magna. Vestibulum vitae dui. Vestibulum nec ligula et lorem consequat ullamcorper.

Listagem A.6: HTML CSS Javascript Code

```
1
2  @media only screen and (min-width: 768px) and (max-width: 991px) {
3
4    #main {
5      width: 712px;
6      padding: 100px 28px 120px;
7    }
8
9    /* .mono {
10     font-size: 90%;
11   } */
12
13   .cssbtn a {
14     margin-top: 10px;
15     margin-bottom: 10px;
16     width: 60px;
17     height: 60px;
18     font-size: 28px;
19     line-height: 62px;
20   }
```

Nulla dui purus, eleifend vel, consequat non, dictum porta, nulla. Duis ante mi, laoreet ut, commodo eleifend, cursus nec, lorem. Aenean eu est. Etiam imperdiet turpis. Praesent nec augue. Curabitur ligula quam, rutrum id, tempor sed, consequat ac, dui. Vestibulum accumsan eros nec magna. Vestibulum vitae dui. Vestibulum nec ligula et lorem consequat ullamcorper.

Listagem A.7: PYTHON Code

```python
class TelgramRequestHandler(object):
    def handle(self):
        addr = self.client_address[0]        # Client IP-adress
        telgram = self.request.recv(1024)    # Recieve telgram
        print "From: %s, Received: %s" % (addr, telgram)
        return
```

B

A Large Table

Aliquam et nisl vel ligula consectetuer suscipit. Morbi euismod enim eget neque. Donec sagittis massa. Vestibulum quis augue sit amet ipsum laoreet pretium. Nulla facilisi. Duis tincidunt, felis et luctus placerat, ipsum libero vestibulum sem, vitae elementum wisi ipsum a metus. Nulla a enim sed dui hendrerit lobortis. Donec lacinia vulputate magna. Vivamus suscipit lectus at quam. In lectus est, viverra a, ultricies ut, pulvinar vitae, tellus. Donec et lectus et sem rutrum sodales. Morbi cursus. Aliquam a odio. Sed tortor velit, convallis eget, porta interdum, convallis sed, tortor. Phasellus ac libero a lorem auctor mattis. Lorem ipsum dolor sit amet, consectetuer adipiscing elit.

Nunc auctor bibendum eros. Maecenas porta accumsan mauris. Etiam enim enim, elementum sed, bibendum quis, rhoncus non, metus. Fusce neque dolor, adipiscing sed, consectetuer et, lacinia sit amet, quam. Suspendisse wisi quam, consectetuer in, blandit sed, suscipit eu, eros. Etiam ligula enim, tempor ut, blandit nec, mollis eu, lectus. Nam cursus. Vivamus iaculis. Aenean risus purus, pharetra in, blandit quis, gravida a, turpis. Donec nisl. Aenean eget mi. Fusce mattis est id diam. Phasellus faucibus interdum sapien. Duis quis nunc. Sed enim. Nunc auctor bibendum eros. Maecenas porta accumsan mauris. Etiam enim enim, elementum sed, bibendum quis, rhoncus non, metus. Fusce neque dolor, adipiscing sed, consectetuer et, lacinia sit amet, quam.

Table B.1: Example table

Benchmark: ANN	#Layers (1)	#Nets (2)	#Nodes* $(3) = 8 \cdot (1) \cdot (2)$	Critical path $(4) = 4 \cdot (1)$	Latency (T_{iter}) (5)
A1	**3–1501**	1	**24–12008**	**12–6004**	4
A2	501	1	4008	2004	**2–2000**
A3	10	**2–1024**	**160–81920**	40	60†
A4	10	50	4000	40	**80–1200**

Benchmark: FFT	FFT size‡ (1)	#Inputs $(2) = 2^{(1)}$	#Nodes* $(3) = 10 \cdot (1) \cdot (2)$	Critical path $(4) = 4 \cdot (1)$	Latency (T_{iter}) (5)
F1	**1–10**	2–1024	**20–102400**	4–40	6–60†
F2	**5**	32	1600	20	**40 – 1500**

Benchmark: Random networks	#Types (1)	#Nodes (2)	#Networks (3)	Critical path (4)	Latency (T_{iter}) (5)
R1	3	10–2000	500	*variable*	(4)
R2	3	50	500	*variable*	$(4) \times [1; \cdots ; 20]$

* *Excluding constant nodes.*
† *Value kept proportional to the critical path:* $(5) = (4) * 1.5$.
‡ *A size of x corresponds to a 2^x point FFT.*
Values in bold indicate the parameter being varied.

As Table B.1 shows, the data can be inserted from a file, in the case of a somehow complex structure. Notice the Table footnotes.

Lorem ipsum dolor sit amet, consectetuer adipiscing elit. Morbi commodo, ipsum sed pharetra gravida, orci magna rhoncus neque, id pulvinar odio lorem non turpis. Nullam sit amet enim. Suspendisse id velit vitae ligula volutpat condimentum. Aliquam erat volutpat. Sed quis velit. Nulla facilisi. Nulla libero. Vivamus pharetra posuere sapien. Nam consectetuer. Sed aliquam, nunc eget euismod ullamcorper, lectus nunc ullamcorper orci, fermentum bibendum enim nibh eget ipsum. Donec porttitor ligula eu dolor. Maecenas vitae nulla consequat libero cursus venenatis. Nam magna enim, accumsan eu, blandit sed, blandit a, eros.

And now an example (Table B.2) of a table that extends to more than one page. Notice the repetition of the Caption (with indication that is continued) and of the Header, as well as the continuation text at the bottom.

Table B.2: Example of a very long table spreading in several pages

Time (s)	Triple chosen	Other feasible triples
0	(1, 11, 13725)	(1, 12, 10980), (1, 13, 8235), (2, 2, 0), (3, 1, 0)
2745	(1, 12, 10980)	(1, 13, 8235), (2, 2, 0), (2, 3, 0), (3, 1, 0)
5490	(1, 12, 13725)	(2, 2, 2745), (2, 3, 0), (3, 1, 0)
8235	(1, 12, 16470)	(1, 13, 13725), (2, 2, 2745), (2, 3, 0), (3, 1, 0)
		Continued on next page

Time (s)	Triple chosen	Other feasible triples
10980	(1, 12, 16470)	(1, 13, 13725), (2, 2, 2745), (2, 3, 0), (3, 1, 0)
13725	(1, 12, 16470)	(1, 13, 13725), (2, 2, 2745), (2, 3, 0), (3, 1, 0)
16470	(1, 13, 16470)	(2, 2, 2745), (2, 3, 0), (3, 1, 0)
19215	(1, 12, 16470)	(1, 13, 13725), (2, 2, 2745), (2, 3, 0), (3, 1, 0)
21960	(1, 12, 16470)	(1, 13, 13725), (2, 2, 2745), (2, 3, 0), (3, 1, 0)
24705	(1, 12, 16470)	(1, 13, 13725), (2, 2, 2745), (2, 3, 0), (3, 1, 0)
27450	(1, 12, 16470)	(1, 13, 13725), (2, 2, 2745), (2, 3, 0), (3, 1, 0)
30195	(2, 2, 2745)	(2, 3, 0), (3, 1, 0)
32940	(1, 13, 16470)	(2, 2, 2745), (2, 3, 0), (3, 1, 0)
35685	(1, 13, 13725)	(2, 2, 2745), (2, 3, 0), (3, 1, 0)
38430	(1, 13, 10980)	(2, 2, 2745), (2, 3, 0), (3, 1, 0)
41175	(1, 12, 13725)	(1, 13, 10980), (2, 2, 2745), (2, 3, 0), (3, 1, 0)
43920	(1, 13, 10980)	(2, 2, 2745), (2, 3, 0), (3, 1, 0)
46665	(2, 2, 2745)	(2, 3, 0), (3, 1, 0)
49410	(2, 2, 2745)	(2, 3, 0), (3, 1, 0)
52155	(1, 12, 16470)	(1, 13, 13725), (2, 2, 2745), (2, 3, 0), (3, 1, 0)
54900	(1, 13, 13725)	(2, 2, 2745), (2, 3, 0), (3, 1, 0)
57645	(1, 13, 13725)	(2, 2, 2745), (2, 3, 0), (3, 1, 0)
60390	(1, 12, 13725)	(2, 2, 2745), (2, 3, 0), (3, 1, 0)
63135	(1, 13, 16470)	(2, 2, 2745), (2, 3, 0), (3, 1, 0)
65880	(1, 13, 16470)	(2, 2, 2745), (2, 3, 0), (3, 1, 0)
68625	(2, 2, 2745)	(2, 3, 0), (3, 1, 0)
71370	(1, 13, 13725)	(2, 2, 2745), (2, 3, 0), (3, 1, 0)
74115	(1, 12, 13725)	(2, 2, 2745), (2, 3, 0), (3, 1, 0)
76860	(1, 13, 13725)	(2, 2, 2745), (2, 3, 0), (3, 1, 0)
79605	(1, 13, 13725)	(2, 2, 2745), (2, 3, 0), (3, 1, 0)
82350	(1, 12, 13725)	(2, 2, 2745), (2, 3, 0), (3, 1, 0)
85095	(1, 12, 13725)	(1, 13, 10980), (2, 2, 2745), (2, 3, 0), (3, 1, 0)
87840	(1, 13, 16470)	(2, 2, 2745), (2, 3, 0), (3, 1, 0)
90585	(1, 13, 16470)	(2, 2, 2745), (2, 3, 0), (3, 1, 0)
93330	(1, 13, 13725)	(2, 2, 2745), (2, 3, 0), (3, 1, 0)
96075	(1, 13, 16470)	(2, 2, 2745), (2, 3, 0), (3, 1, 0)
98820	(1, 13, 16470)	(2, 2, 2745), (2, 3, 0), (3, 1, 0)
101565	(1, 13, 13725)	(2, 2, 2745), (2, 3, 0), (3, 1, 0)
104310	(1, 13, 16470)	(2, 2, 2745), (2, 3, 0), (3, 1, 0)
107055	(1, 13, 13725)	(2, 2, 2745), (2, 3, 0), (3, 1, 0)
109800	(1, 13, 13725)	(2, 2, 2745), (2, 3, 0), (3, 1, 0)
112545	(1, 12, 16470)	(1, 13, 13725), (2, 2, 2745), (2, 3, 0), (3, 1, 0)
115290	(1, 13, 16470)	(2, 2, 2745), (2, 3, 0), (3, 1, 0)
118035	(1, 13, 13725)	(2, 2, 2745), (2, 3, 0), (3, 1, 0)
120780	(1, 13, 16470)	(2, 2, 2745), (2, 3, 0), (3, 1, 0)
123525	(1, 13, 13725)	(2, 2, 2745), (2, 3, 0), (3, 1, 0)
126270	(1, 12, 16470)	(1, 13, 13725), (2, 2, 2745), (2, 3, 0), (3, 1, 0)
129015	(2, 2, 2745)	(2, 3, 0), (3, 1, 0)
131760	(2, 2, 2745)	(2, 3, 0), (3, 1, 0)
134505	(1, 13, 16470)	(2, 2, 2745), (2, 3, 0), (3, 1, 0)
137250	(1, 13, 13725)	(2, 2, 2745), (2, 3, 0), (3, 1, 0)
139995	(2, 2, 2745)	(2, 3, 0), (3, 1, 0)
142740	(2, 2, 2745)	(2, 3, 0), (3, 1, 0)
145485	(1, 12, 16470)	(1, 13, 13725), (2, 2, 2745), (2, 3, 0), (3, 1, 0)

Table B.2 – continued from previous page

Time (s)	Triple chosen	Other feasible triples
148230	(2, 2, 2745)	(2, 3, 0), (3, 1, 0)
150975	(1, 13, 16470)	(2, 2, 2745), (2, 3, 0), (3, 1, 0)
153720	(1, 12, 13725)	(2, 2, 2745), (2, 3, 0), (3, 1, 0)
156465	(1, 13, 13725)	(2, 2, 2745), (2, 3, 0), (3, 1, 0)
159210	(1, 13, 13725)	(2, 2, 2745), (2, 3, 0), (3, 1, 0)
161955	(1, 13, 16470)	(2, 2, 2745), (2, 3, 0), (3, 1, 0)
164700	(1, 13, 13725)	(2, 2, 2745), (2, 3, 0), (3, 1, 0)

An example of a large Table that autofits the size to the page margins is illustrated in Table B.3. Please notice the text size that is shrunken in order fot the table to adjust to the page:

Table B.3: Sample Table.

URL	First Time Visit	Last Time Visit	URL Counts	Value	Reference
https://web.facebook.com/	1521241972	1522351859	177	56640	[facebook-2021]
http://localhost/phpmyadmin/	1518413861	1522075694	24	39312	database-management
https://mail.google.com/mail/u/	1516596003	1522352010	36	33264	Google-Gmail-2021
https://github.com/shawon100	1517215489	1522352266	37	27528	Code-Repository
https://www.youtube.com/	1517229227	1521978502	24	14792	Youtube-video-2021